NMR of Solids

J. Fraissard

University P. and M. Curie, Paris
ESPCI
Laboratory « Physique et Etude de Matériaux »

Interactions of nuclear spins in a solid

-:-:-:-:-:-:-:-

$\hat{H}_Z$ = Zeeman effect $\hat{H}_{RF}$ = RF field $\hat{H}_{CS}$ = Chemical shift $\hat{H}_J$ = JJ coupling $\hat{H}_D$ = Dipole interactions $\hat{H}_Q$ = Quadrupole coupling $\hat{H}_{ij}$ = Unpaired electron	$\hat{H}_X = \vec{A}\ \overline{T_X}\ \vec{B}$ $\overline{T_X}$=second rank tensor

$\hat{H}_Z >>$ other interactions

Very often some effects are masked by the others.
For example $\hat{H}_D >> \hat{H}_J$

$\hat{H}_X$ = K (spin factor) [space factor f(θ)]

θ = angle between an axis of the system and B_0

Chemical Shift

Chemical shift δ

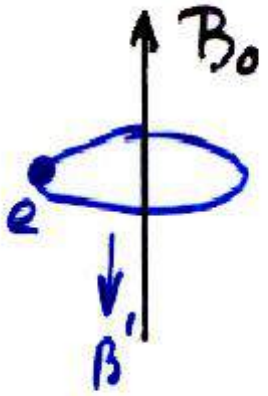

$$\omega = \gamma B$$

Sample: $2\pi\nu_s = \gamma B_0(1-\sigma_s)$

Reference: $2\pi\nu_r = \gamma B_0(1-\sigma_r)$

$$\Delta\nu = \nu_r - \nu_s = \frac{\gamma B_0}{2\pi}(\sigma_s - \sigma_r)$$

$$\delta = \frac{\gamma B_0/2\pi\,(\sigma_s - \sigma_r)}{\gamma B_0/2\pi\,(1-\sigma_r)} \sim \sigma_s - \sigma_r \quad \text{p/m}$$

SPIN-SPIN COUPLING J

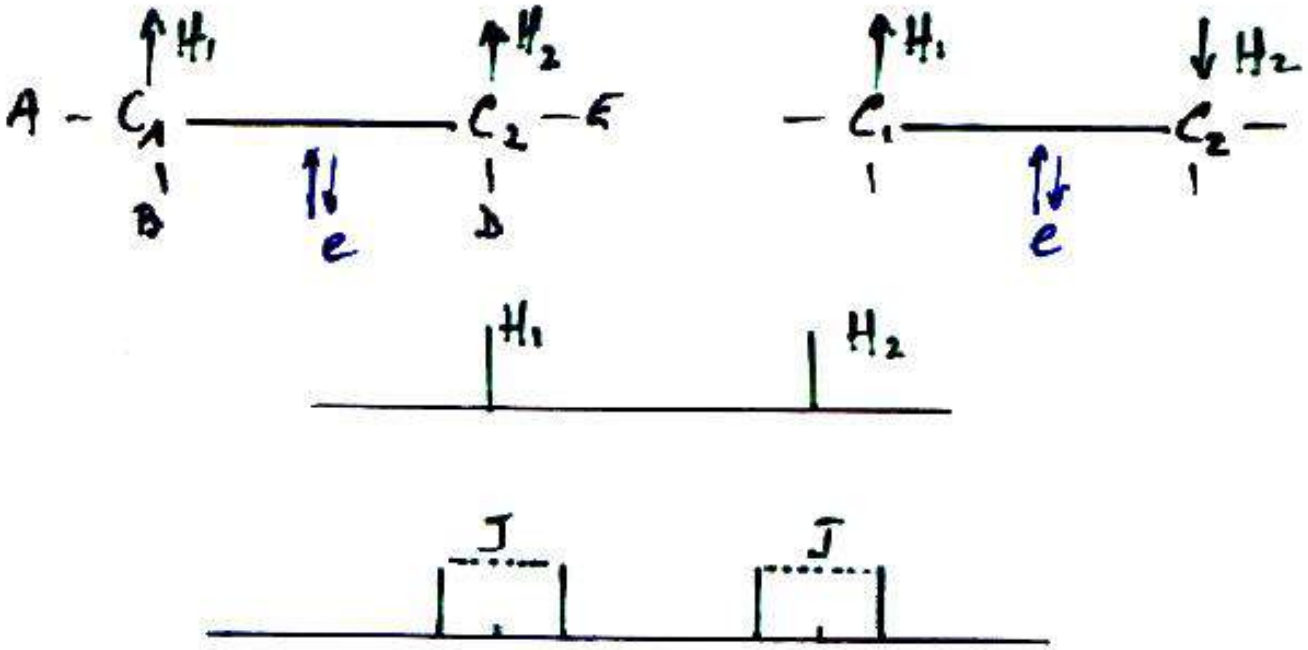

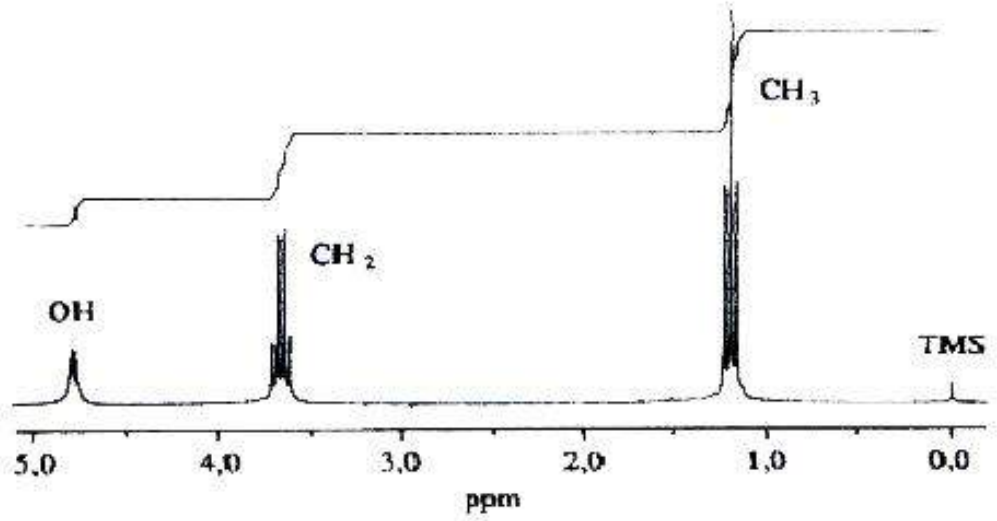

2 n I + 1

Ethyl acetate

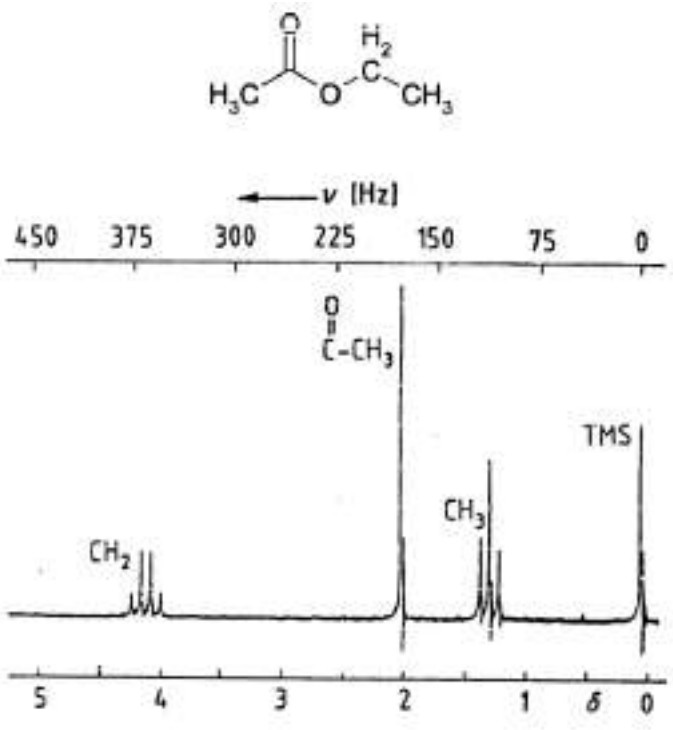

Dipolar Magnetic Interaction between two ^{1}H nuclei

$$DMI = CONSTANT \cdot (1 - 3\cos^2\theta) \cdot r^{-3}$$

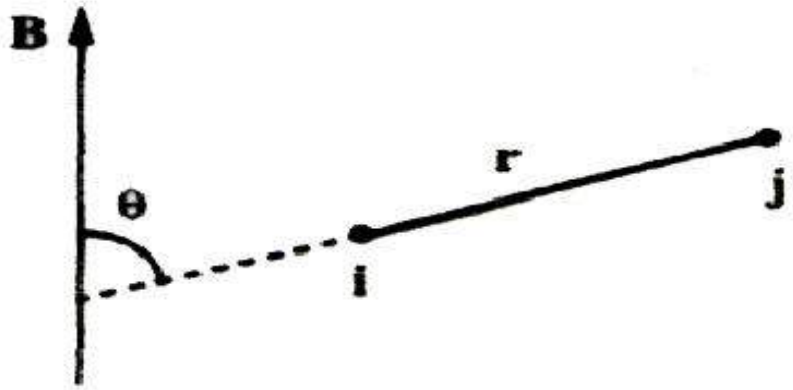

For powder samples the interactions must be summer up over all directions.

DMI = 0 if $\cos\theta = 1/\sqrt{3}$

θ = 54° 44'

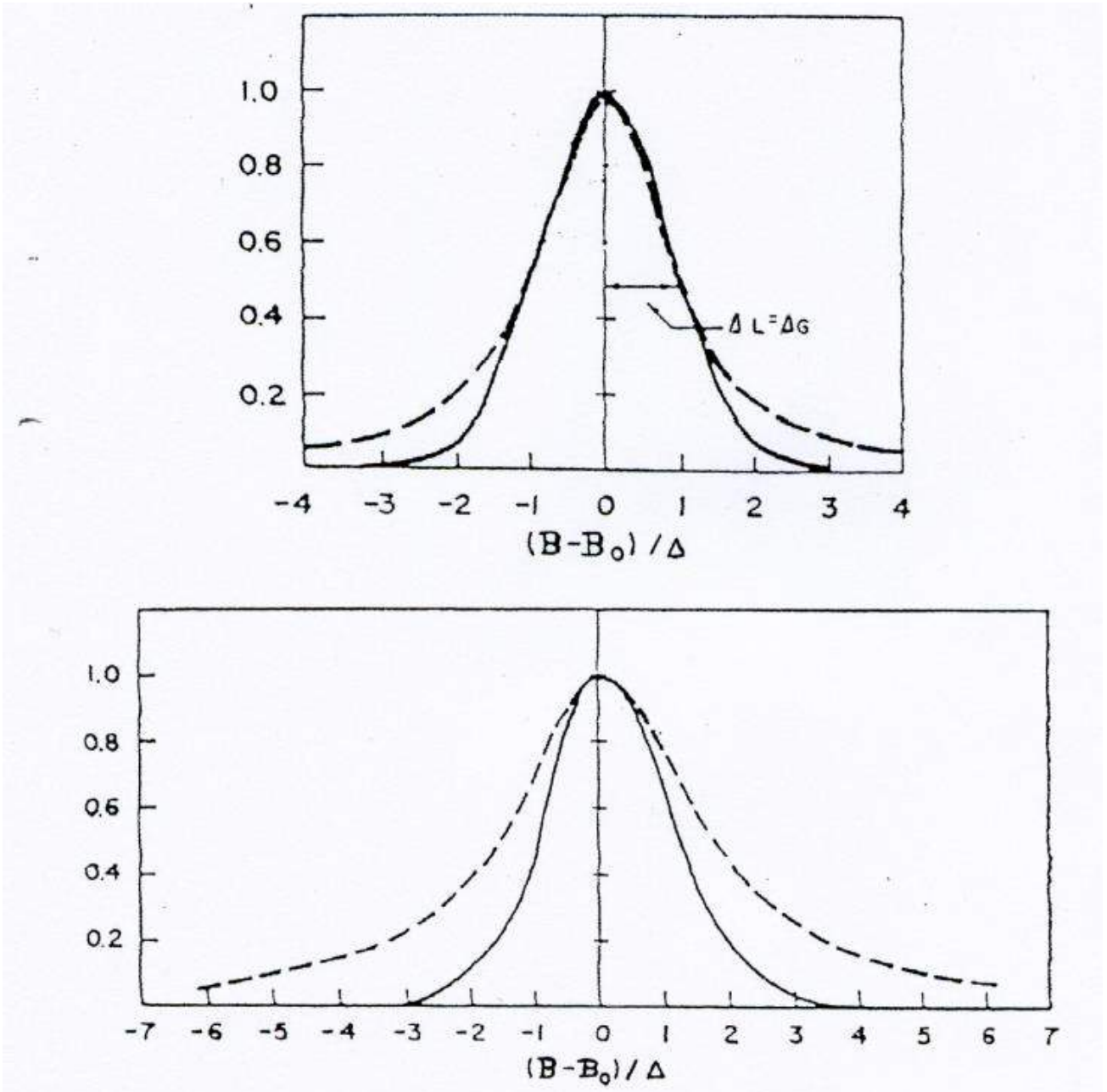

Figure 1. Zero derivative curves for Gaussian (solid line) and Lorentzi (broken line) shape function; (a) curves have the same half-line width half-maximum intensity; (b) curves have the same peak-to-peak li width.

Spectrum for a two spins magnetic configuration

- - - - - theoretical; _____ real

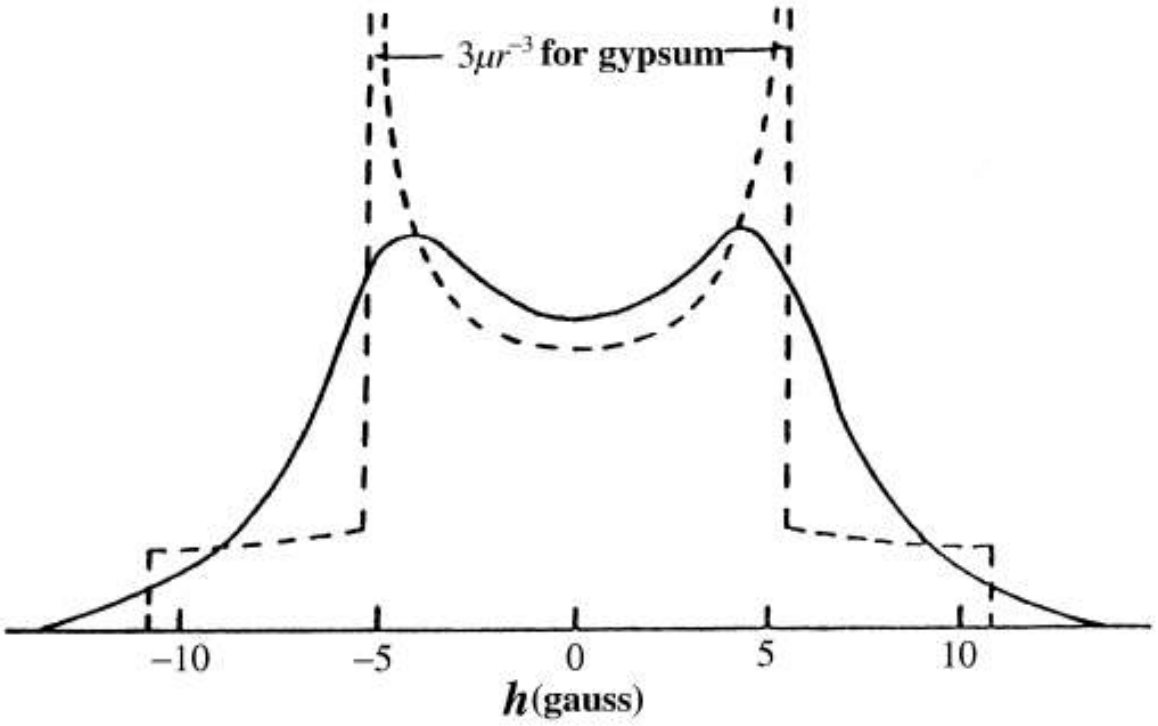

FIG. 3.10 – Spectres théorique (courbe en pointillée) et réel (trait plein) pour une configuration magnétique à deux spins dans une poudre.

Magic angle spinning (MAS)

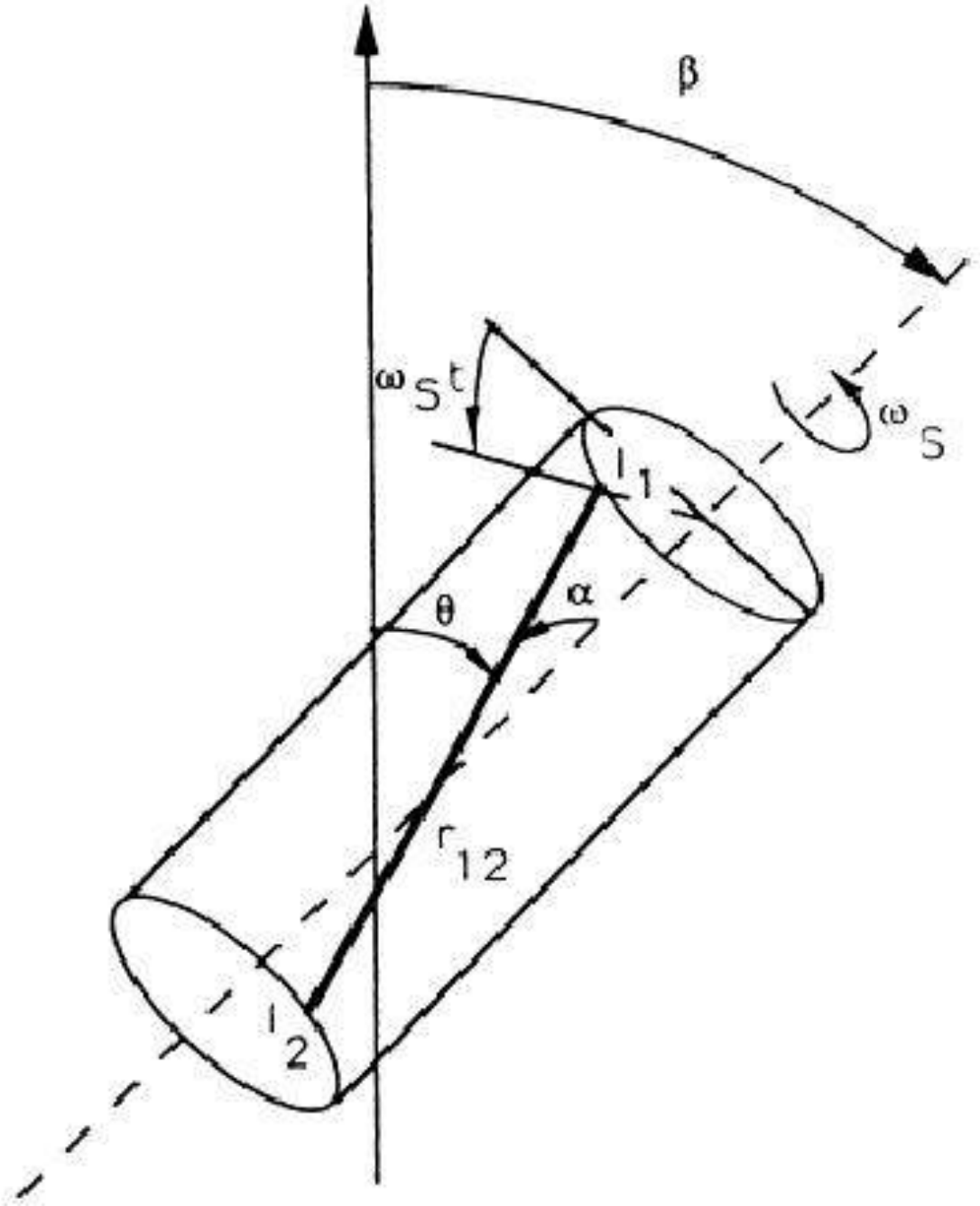

The angle between the diagonal of the cube and the side is = the magic angle

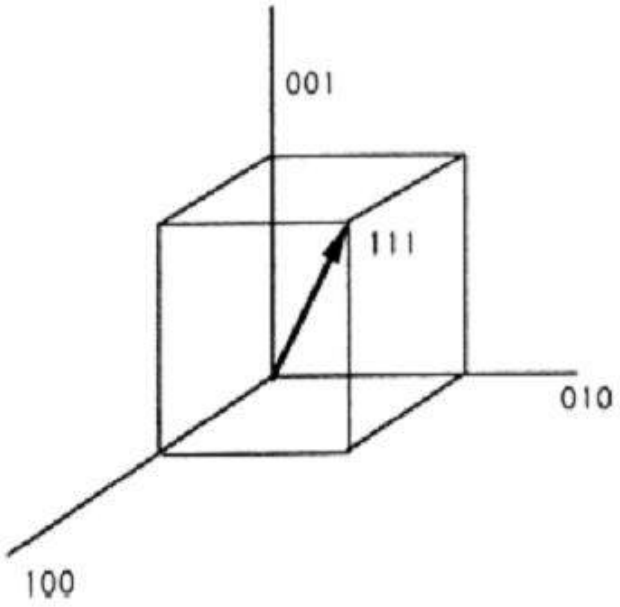

Pulse sequences

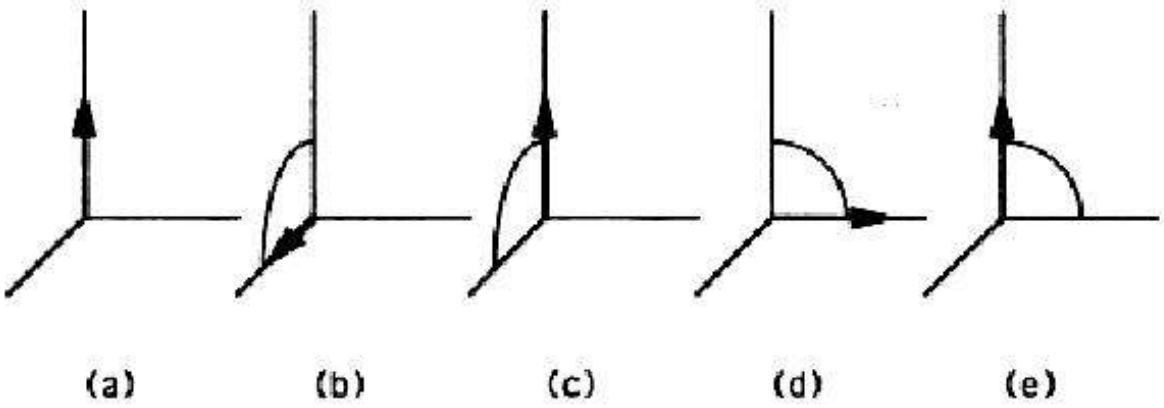

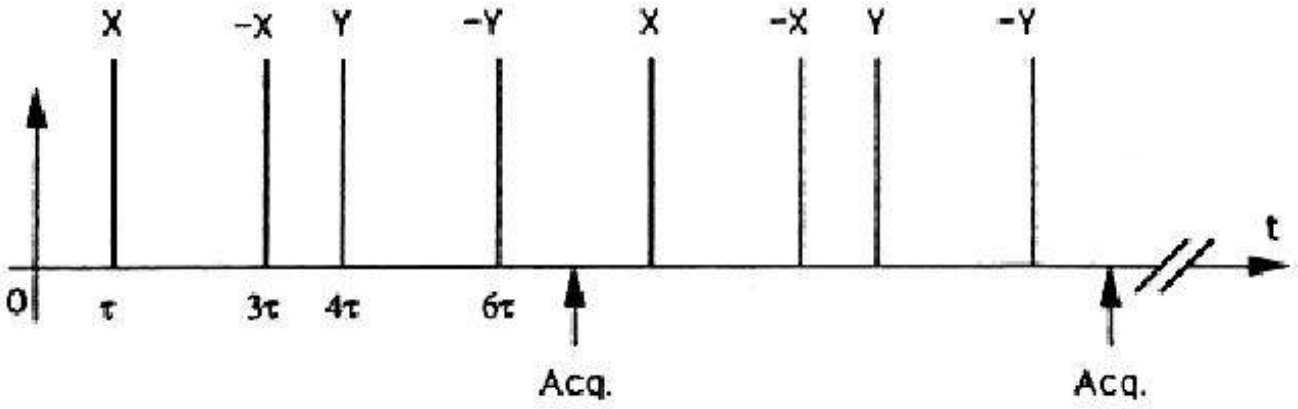

^{19}F NMR. Application of the Wahuha sequence to perfluorocyclohexane C_6F_{12} at 200 K

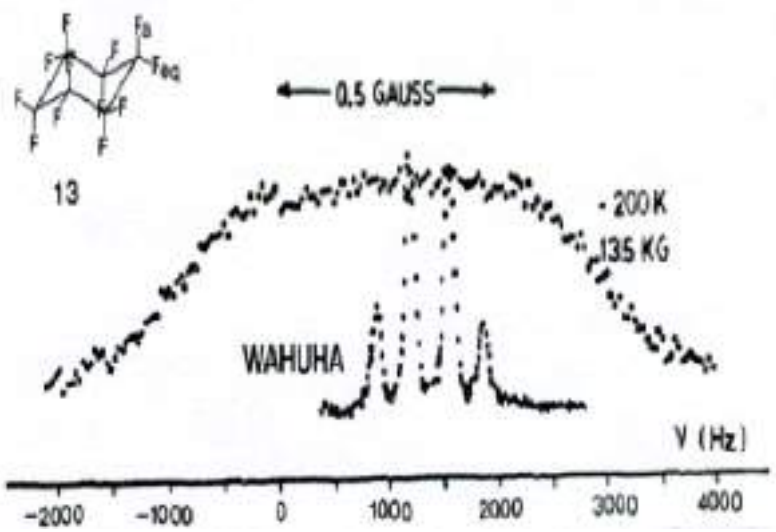

4.4’-dimethylbenzophenol

A: MREV-8; B: MREV-8 + MAS; C: BR24 + MAS

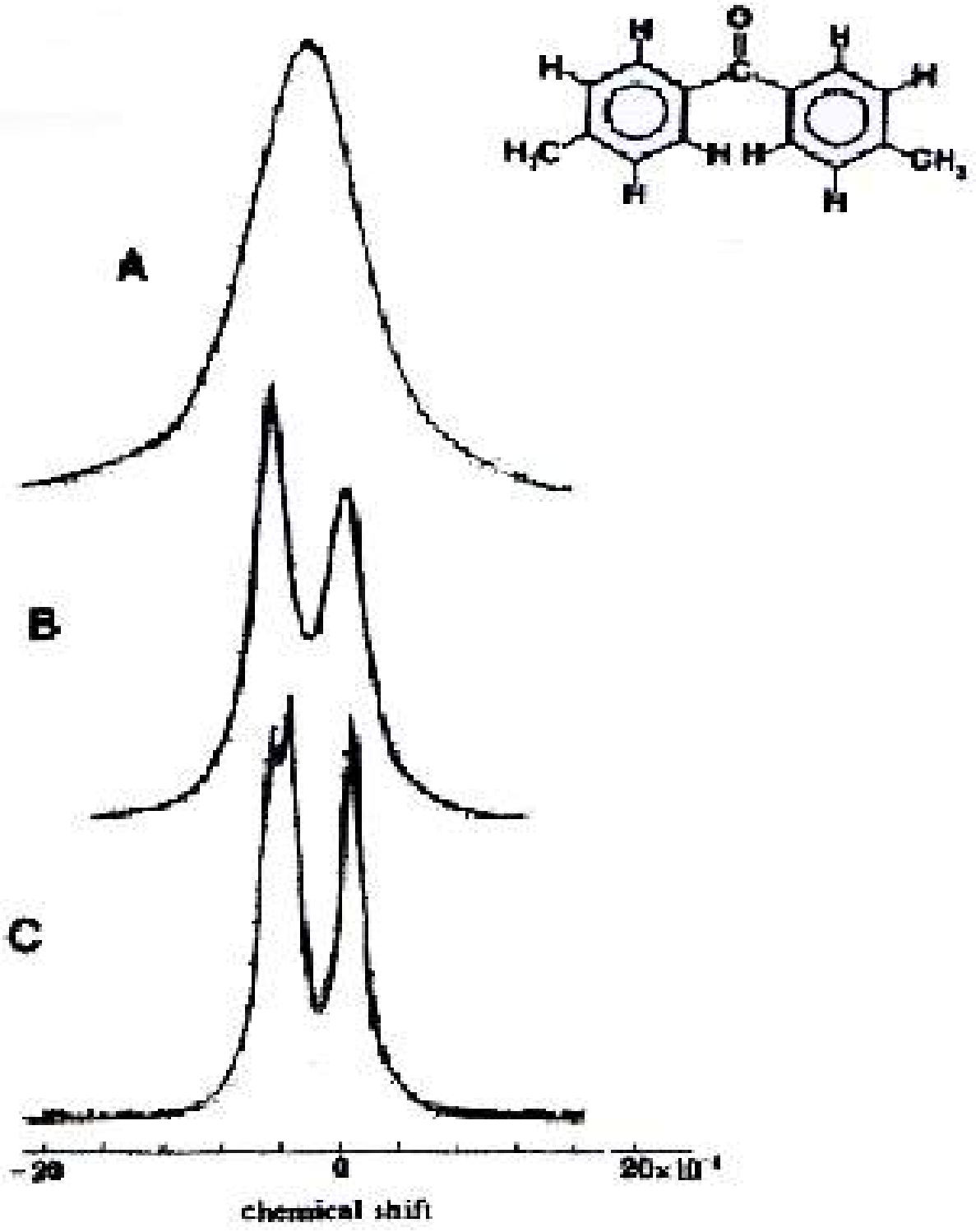

IR: $\Delta\nu$ in cm^{-1} against hydrogen bond

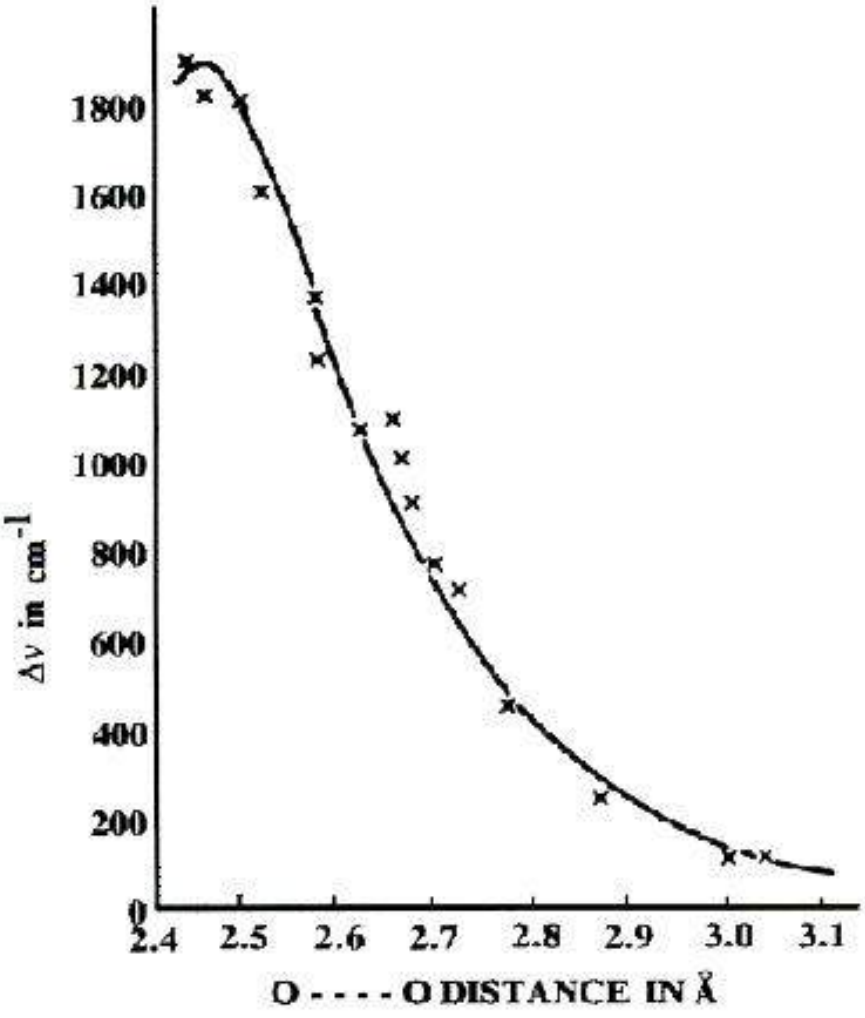

The relation between OH frequency shift and O - - - - O distance during hydrogen-bonding interaction

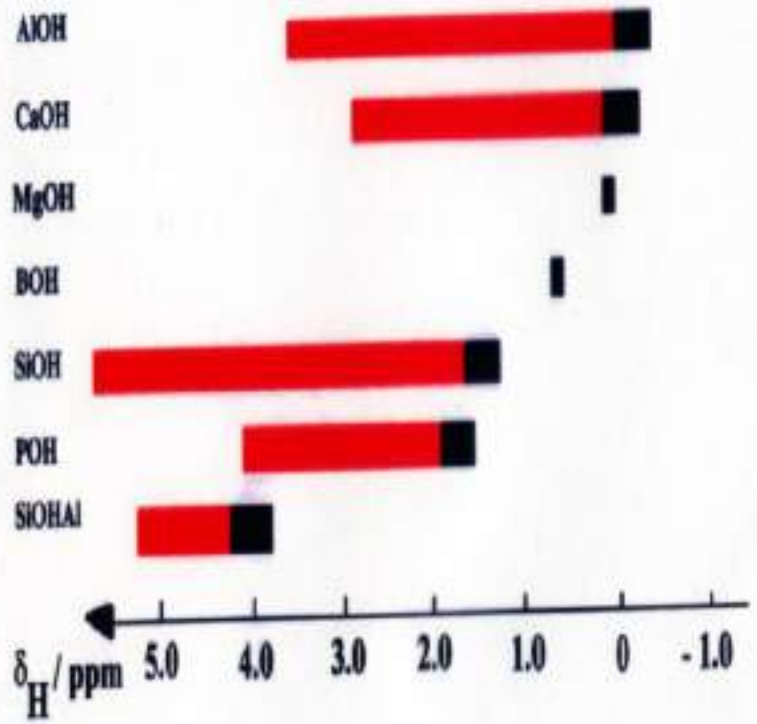

Intervals for the experimentally determined values of the ^1H NMR chemical shift δ_H of isolated (black) and interacting (red area) OH groups in zeolites.

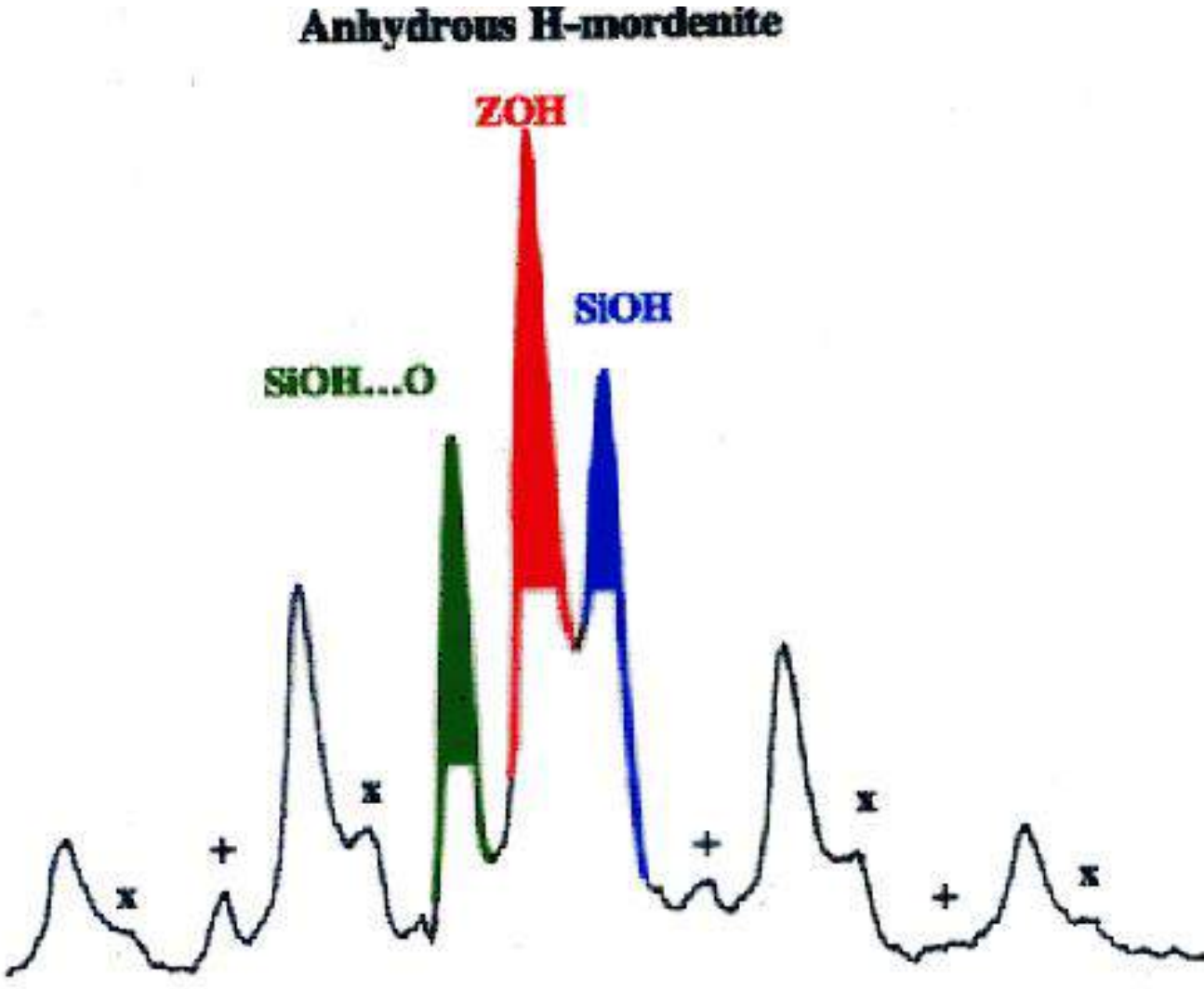
Anhydrous H-mordenite
ZOH
SiOH
SiOH...O
x
+
x
+
x
+
x

Maleic acid at 60 and 270 MHz
Influence of hydrogen bond
$HO_2CHC=CHCO_2H$

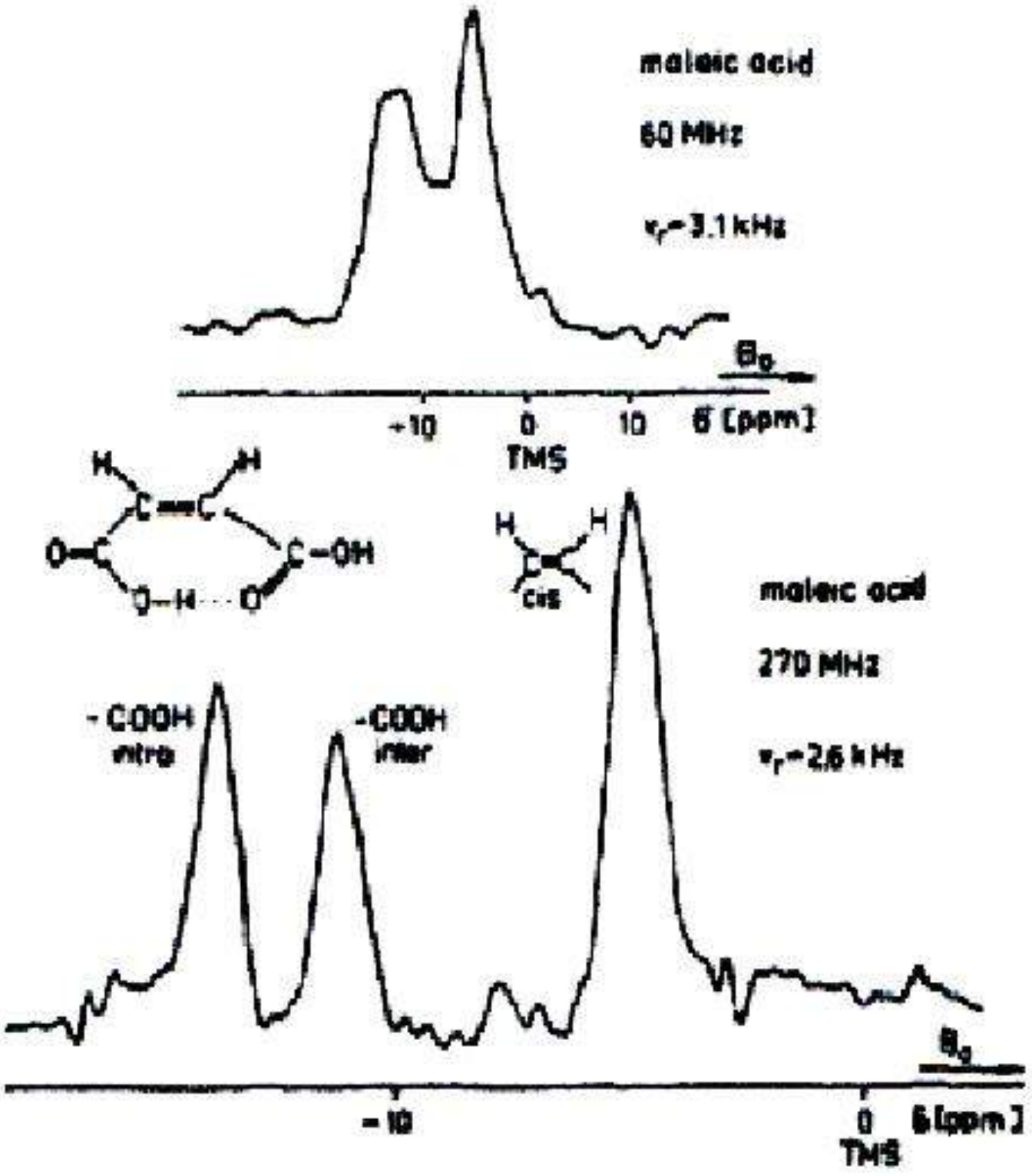

Poly phenylene oxide and blend with polystyrene

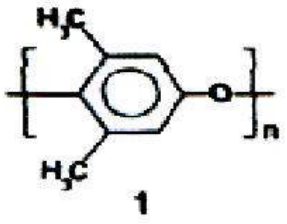

1

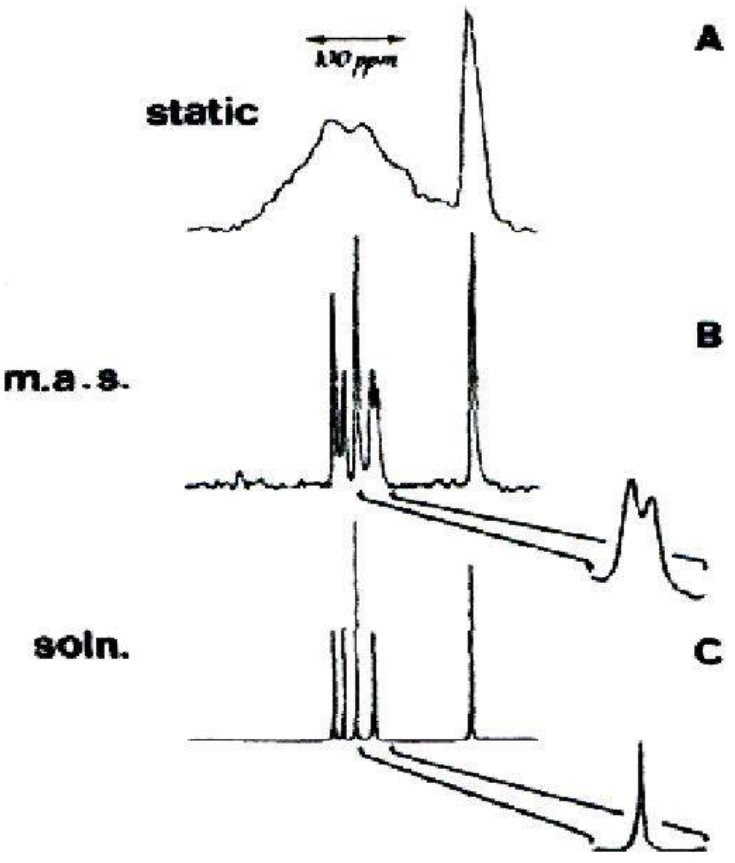

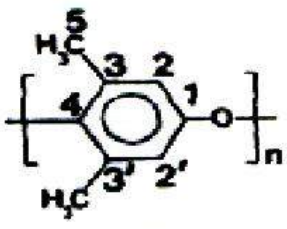

1

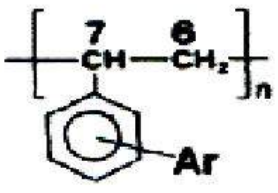

2

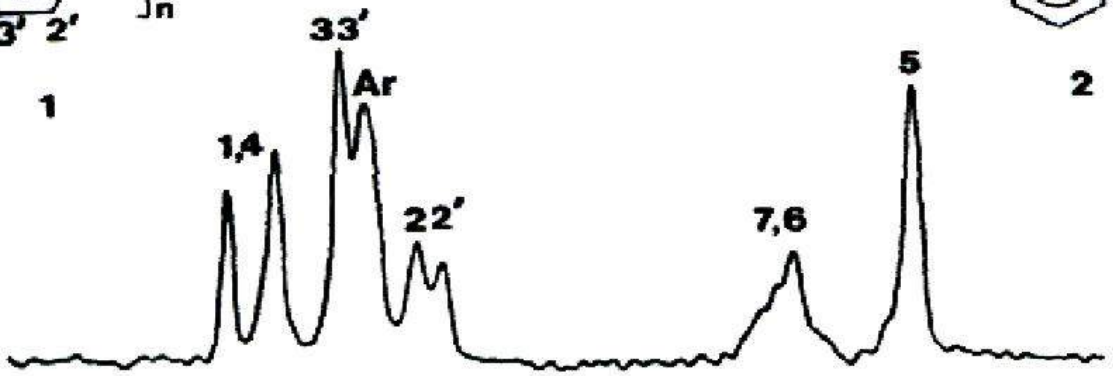

Hydrogen bonds: δ (OH) and ν (OH) comparison of intensities

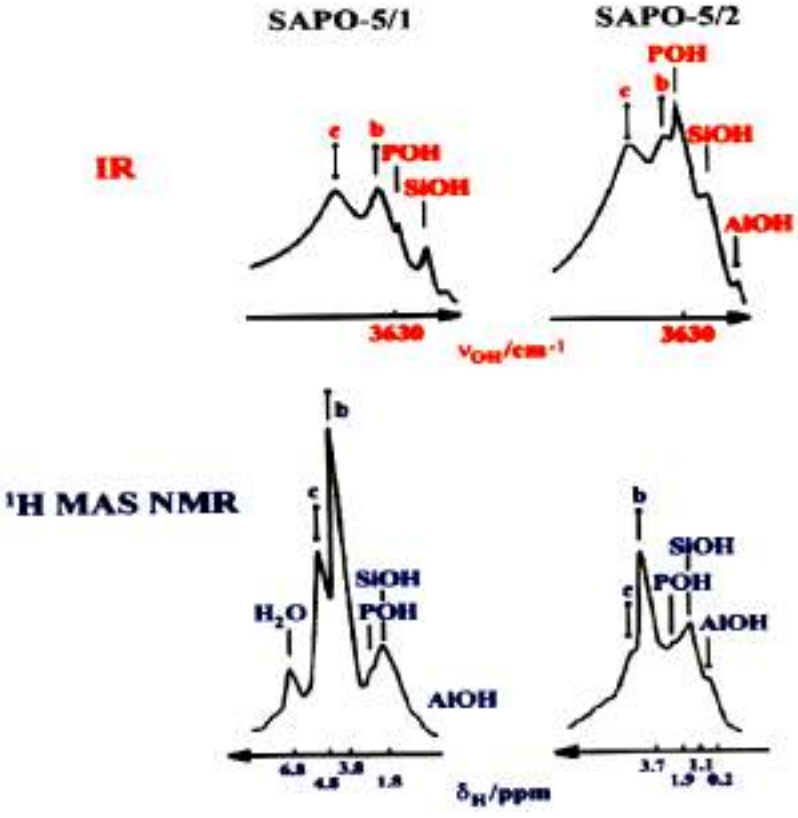

Polarization transfer from abundant spins I (high γ_I) to the low concentration spins S (low γ_S)

-:-:-:-:-:-:-

For spins ½,
magnetization : $M = (N/4k_BT)\,\gamma\hbar B_0$

Signal/ noise ratio: $\propto (I+1)\,N\gamma^{5/2}$

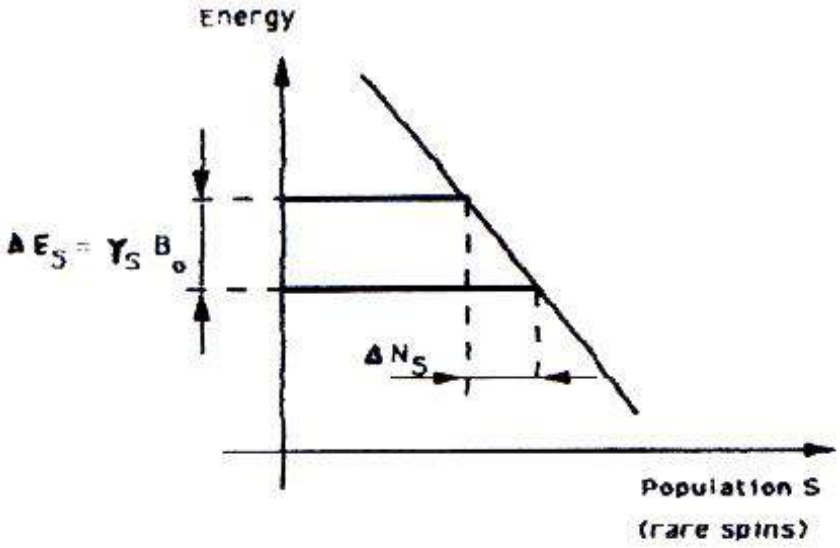

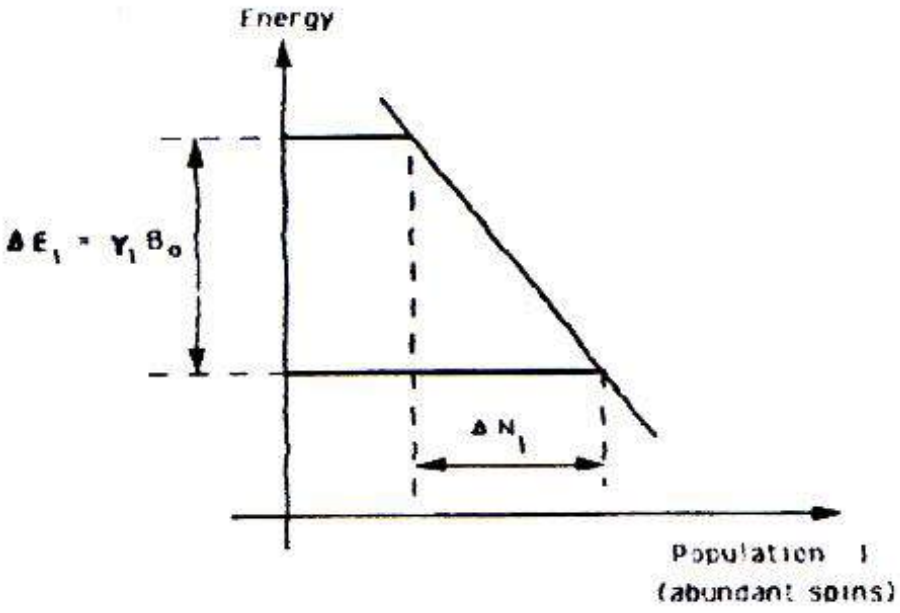

For the same B_0, ΔN_I and ΔN_S are proportional to γ_I and γ_S.

$\Delta N_I/\Delta N_S = \gamma_I/\gamma_S$

In the rotating framework
B_{1I} along x' $\rightarrow$rotation of M_I in the plane zoy'

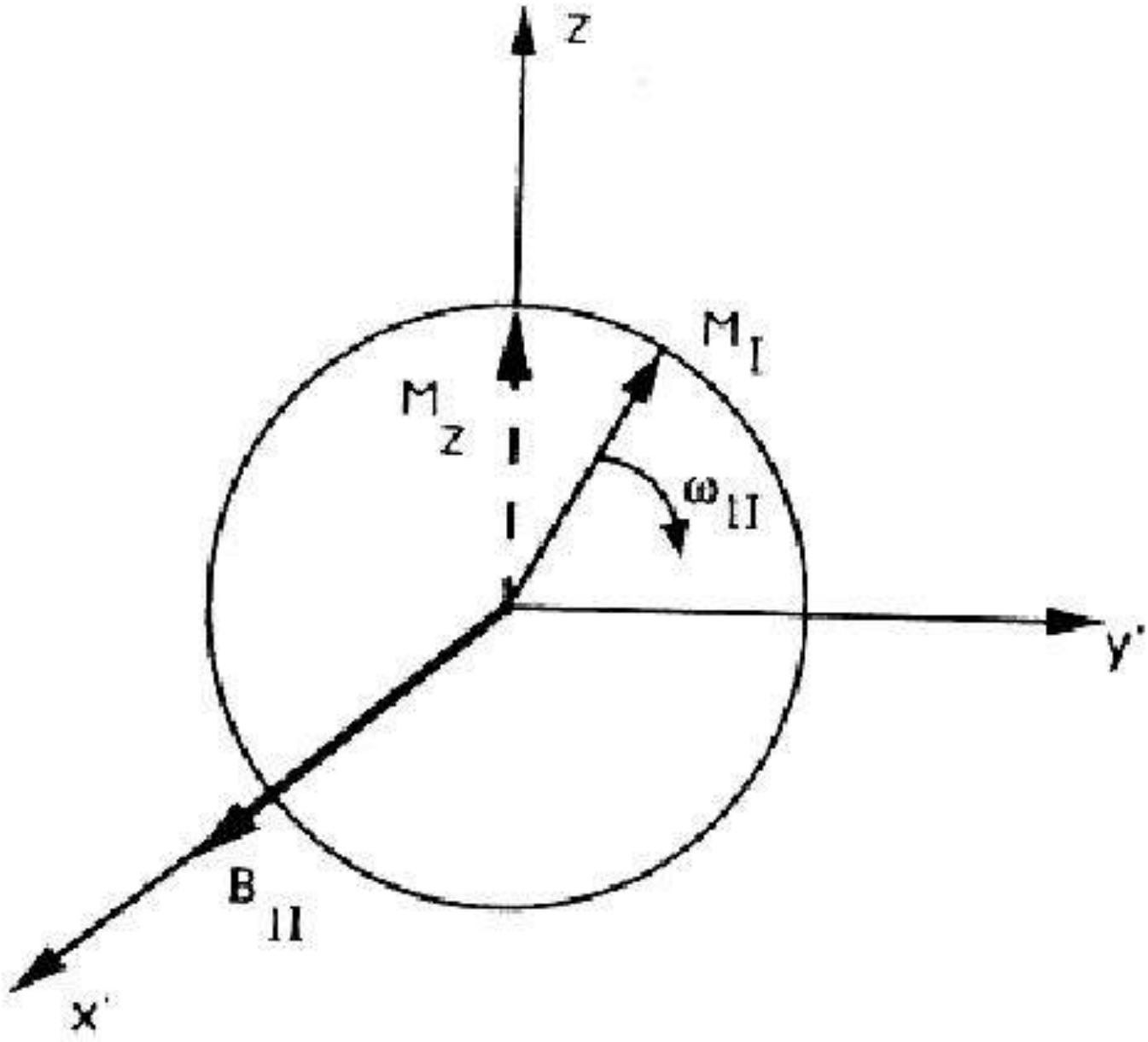

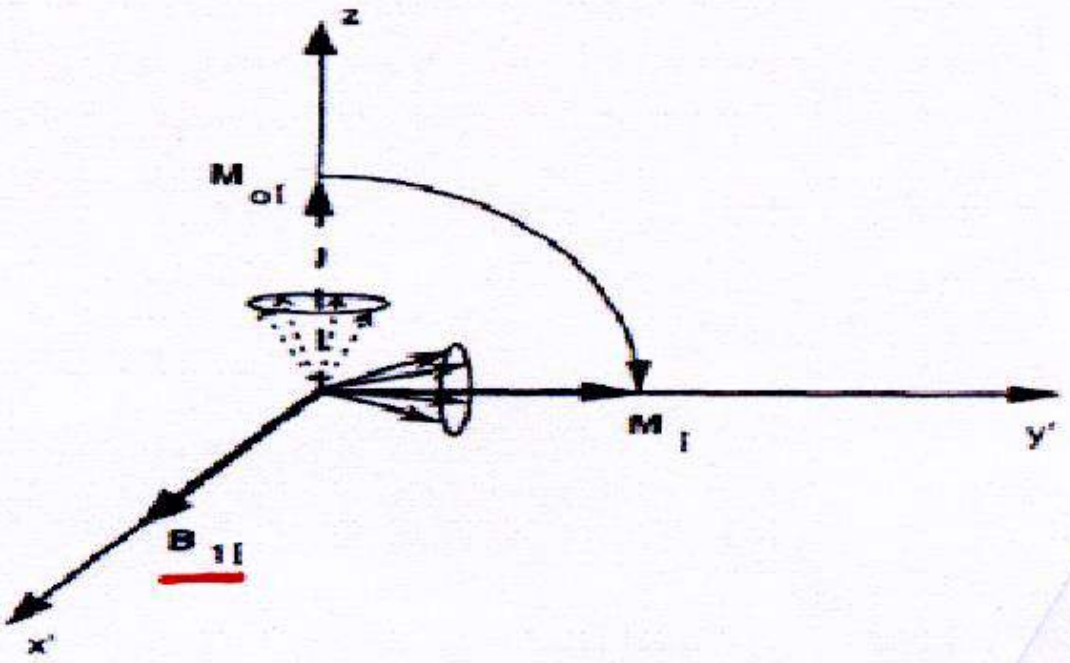

After a $\pi/2$ pulse along x' at frequency ω_{0I} the abundant spin magnetization M_I lies along y'.

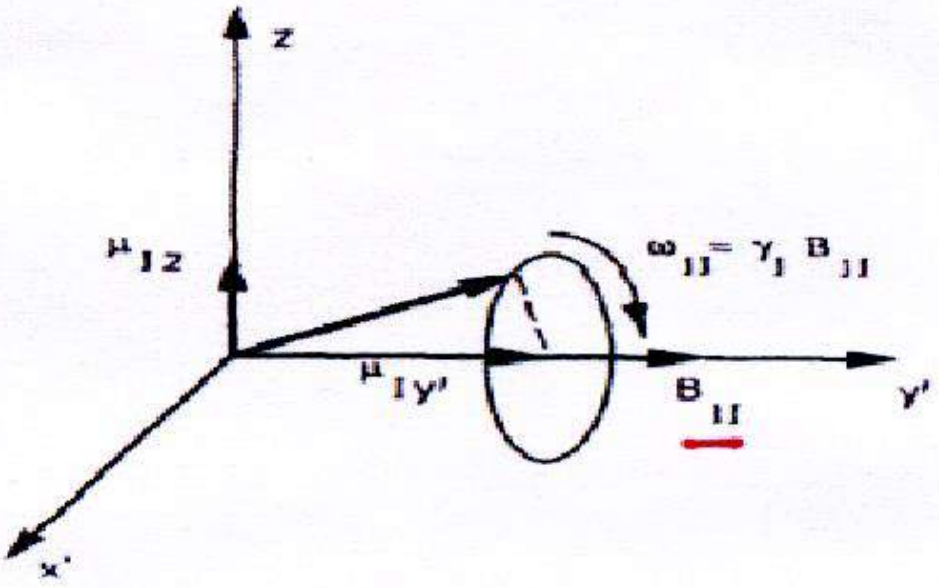

Immediately after a second $\pi/2$ pulse along y' the I spins rotate around y'. The resultant magnetization M_I is "spin-locked" on the axis.

Due to another rf field $B_{1,S}$ along X', individual magnetic moment μ_S turns around X' with a frequency $\omega_{1,S}=\gamma_S B_{1,S}$

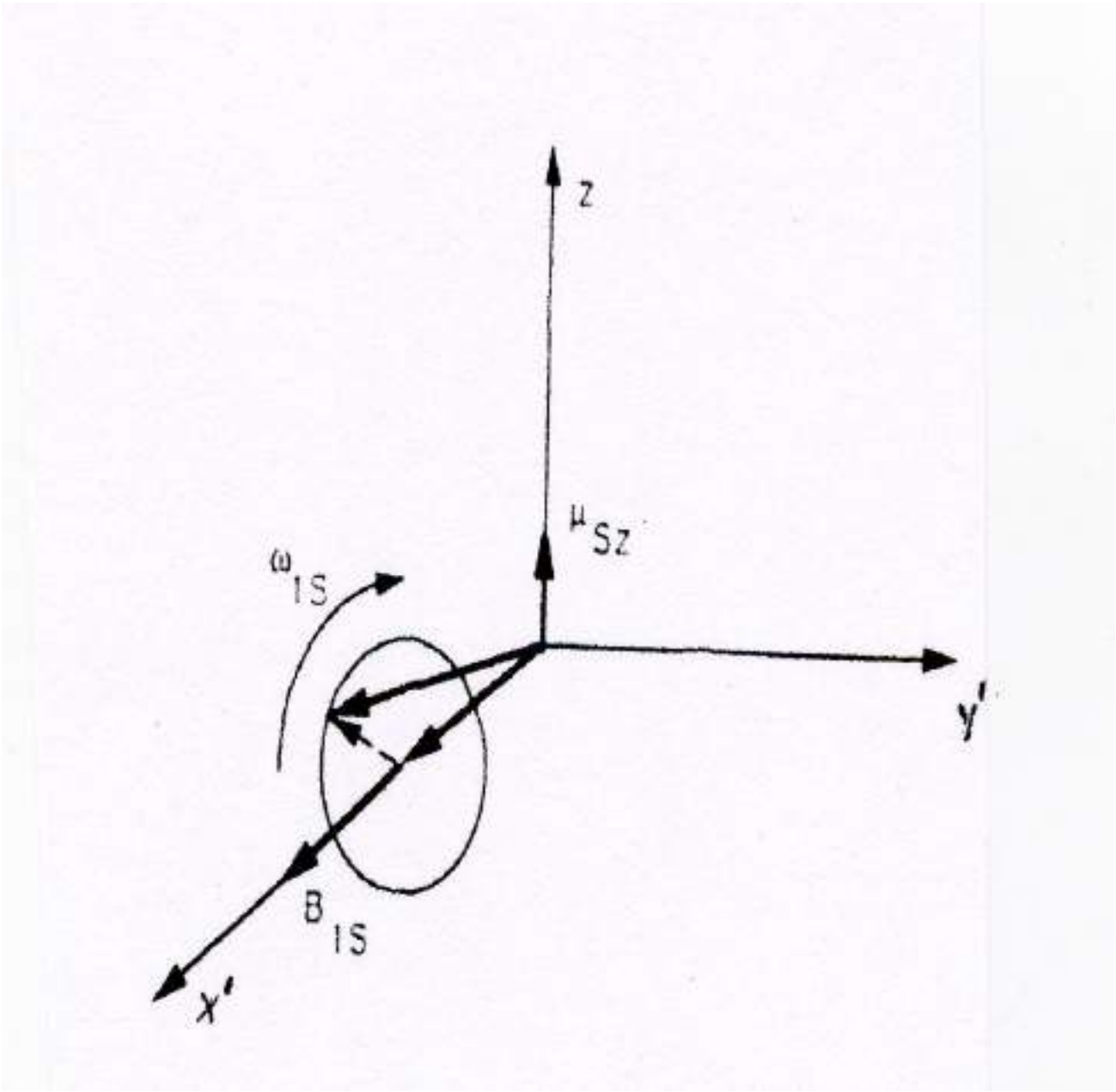

Hartmann-Hahn condition

I and S have the oscillating components which may have the same time dependence if

$$\omega_{1I} = \omega_{1S}$$

$$\gamma_S B_{1S} = \gamma_I B_{1I}$$

^{13}C NMR of Pyridine
a: liquid (left)and in H_2SO_4(right)
b and c:adsorbed on NaY(left) and HY(right)

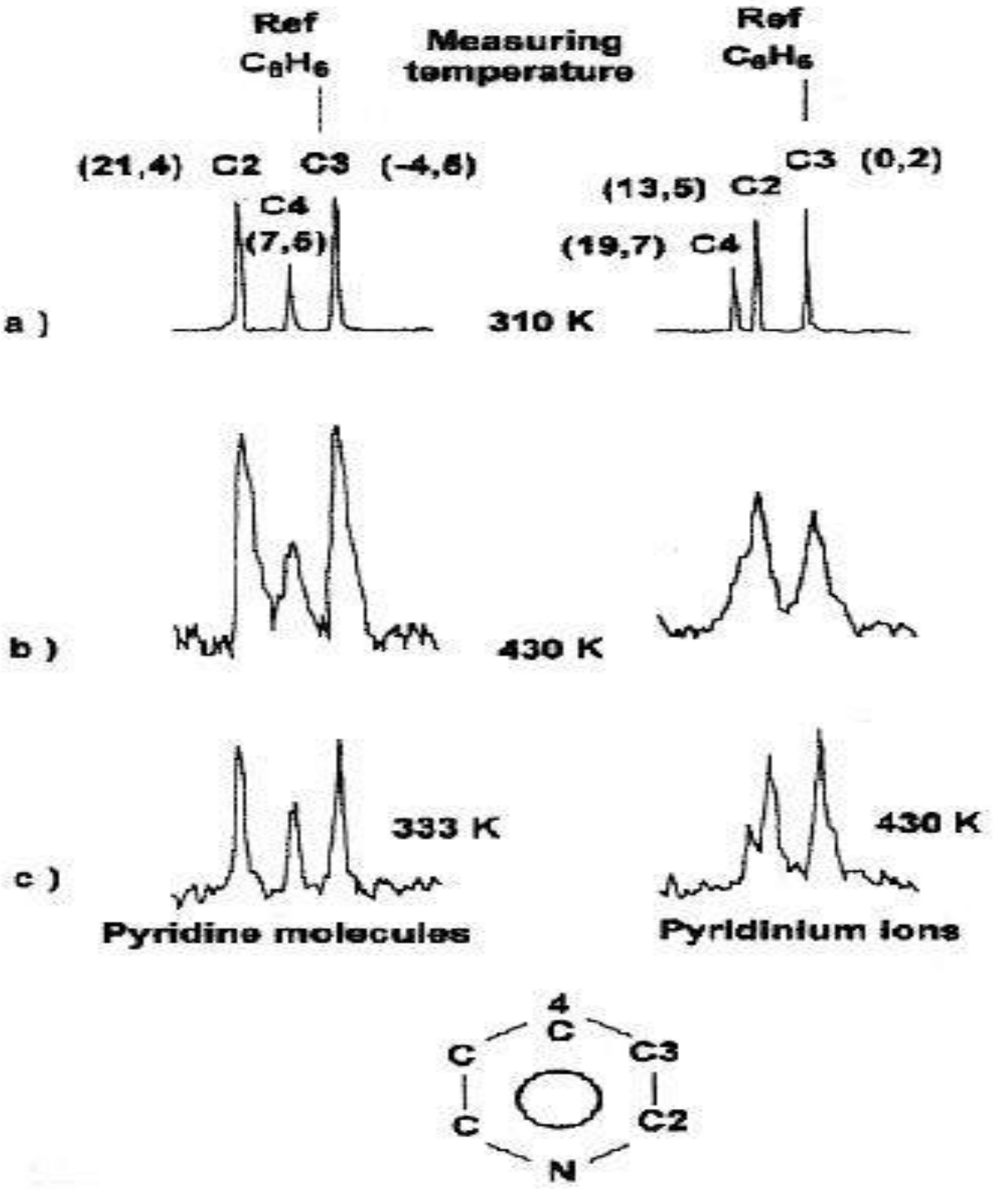

$\delta(^{29}Si)$ for silicates Q_n

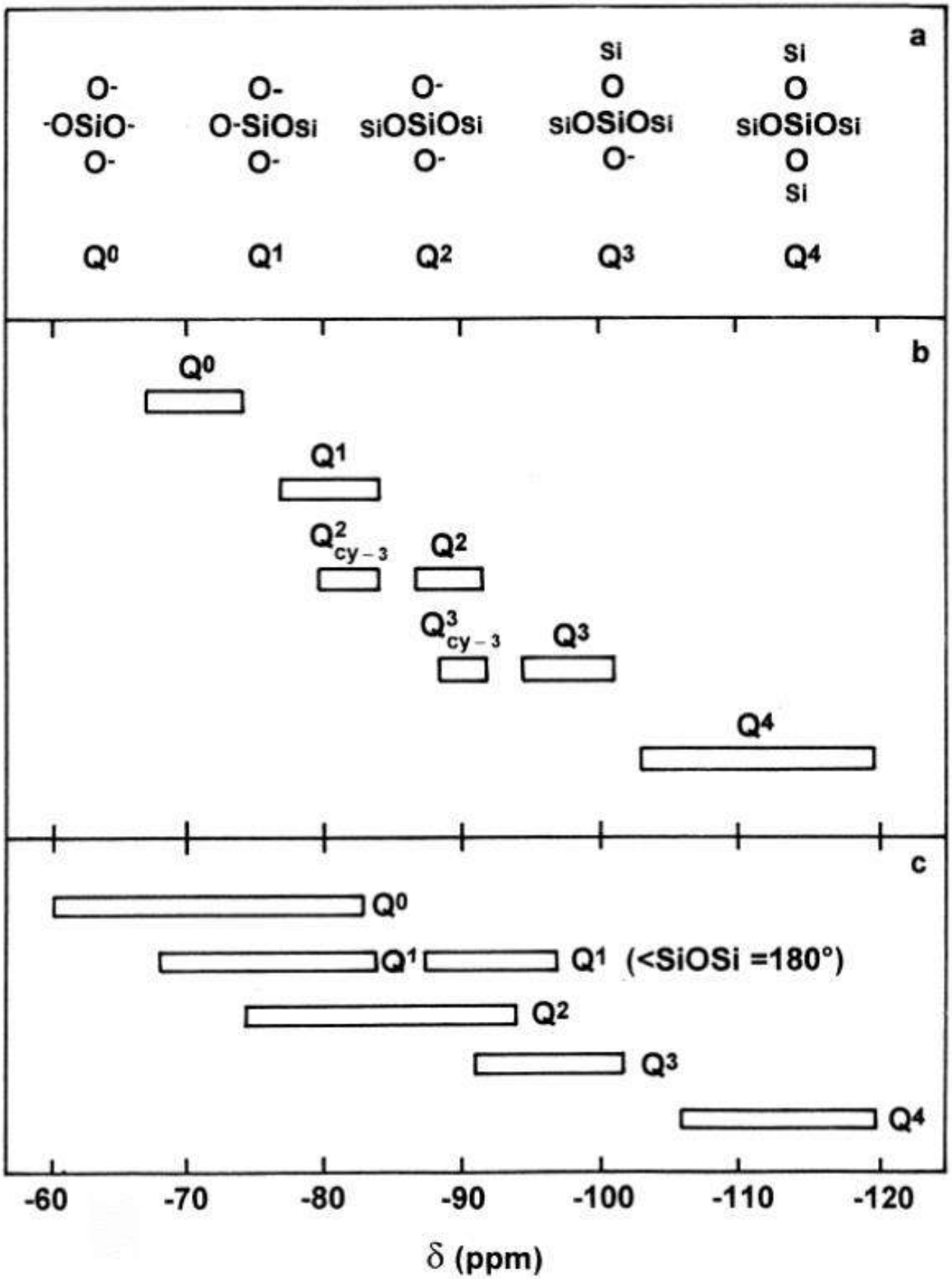

δ (Si)

Xonolite Tremolite

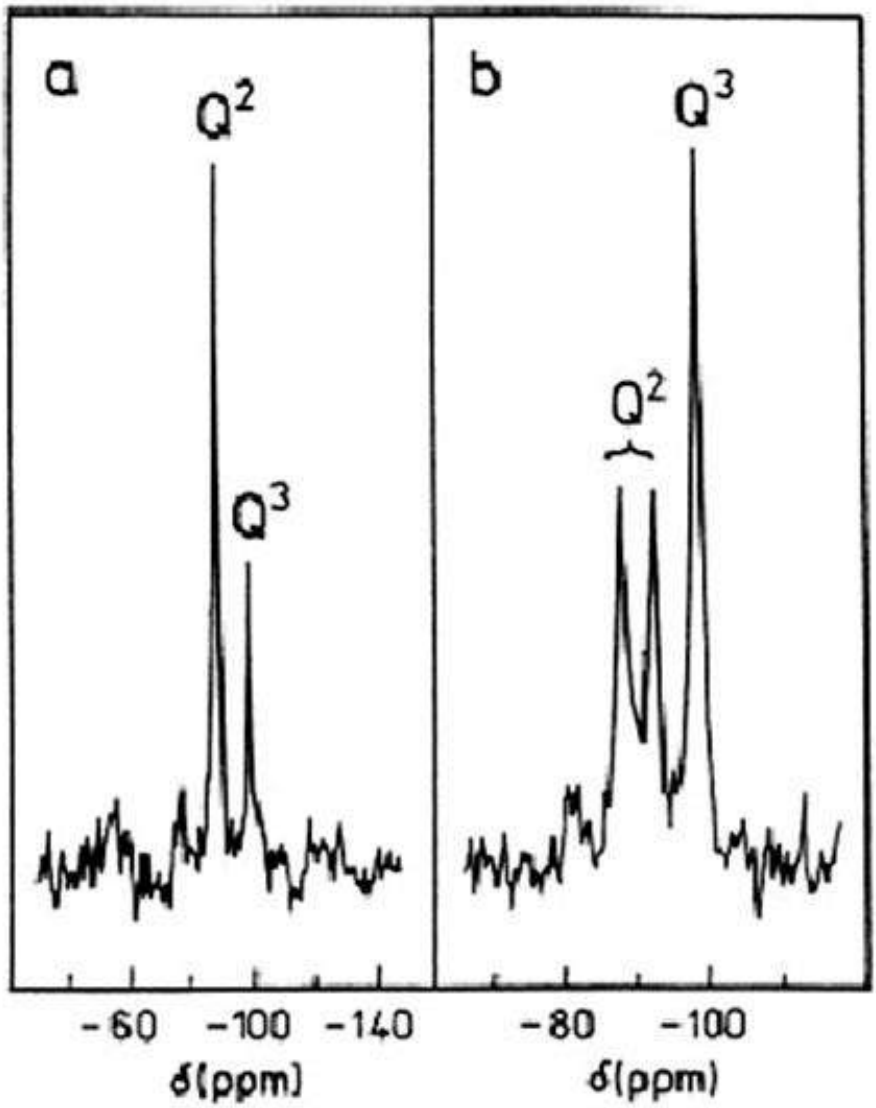

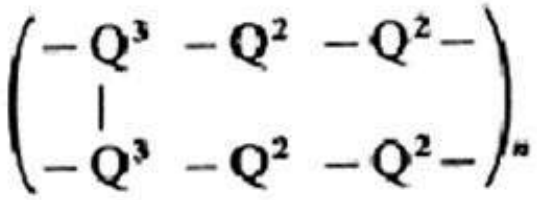

Xonolite $Ca_6Si_6O_{17}(OH)_2$

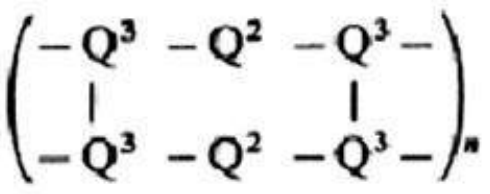

tremolite $Ca_2Mg_5(Si_4O_{11})_2(OH)_2$

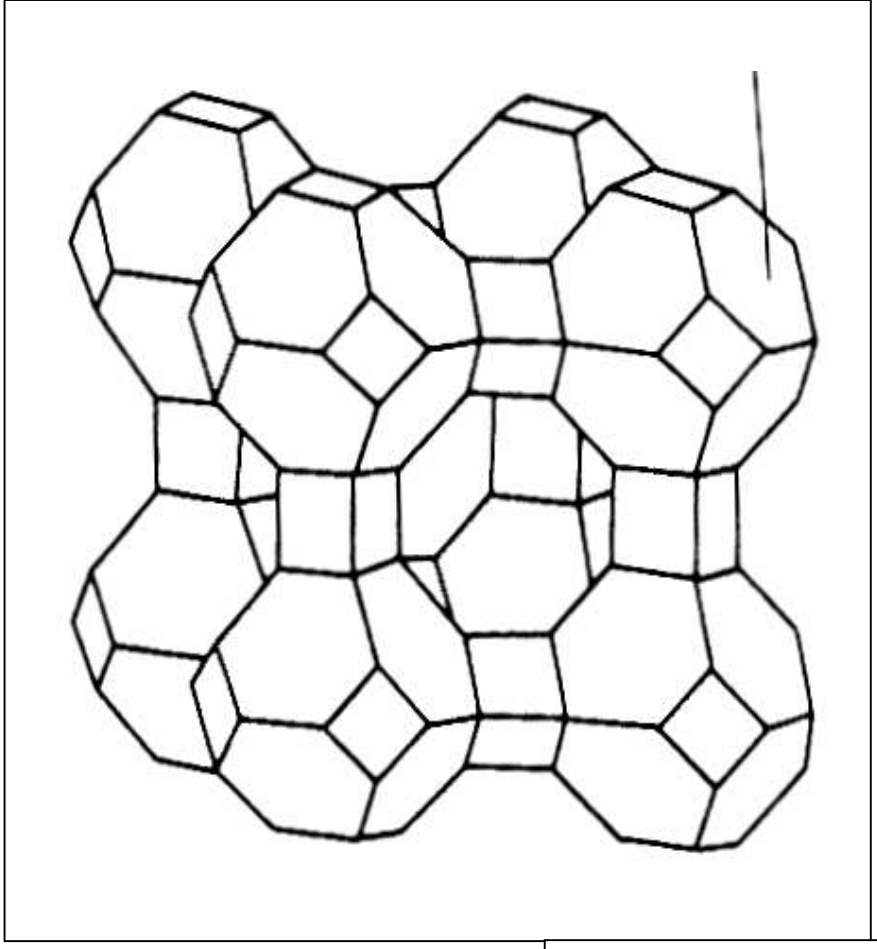

Zeolite A

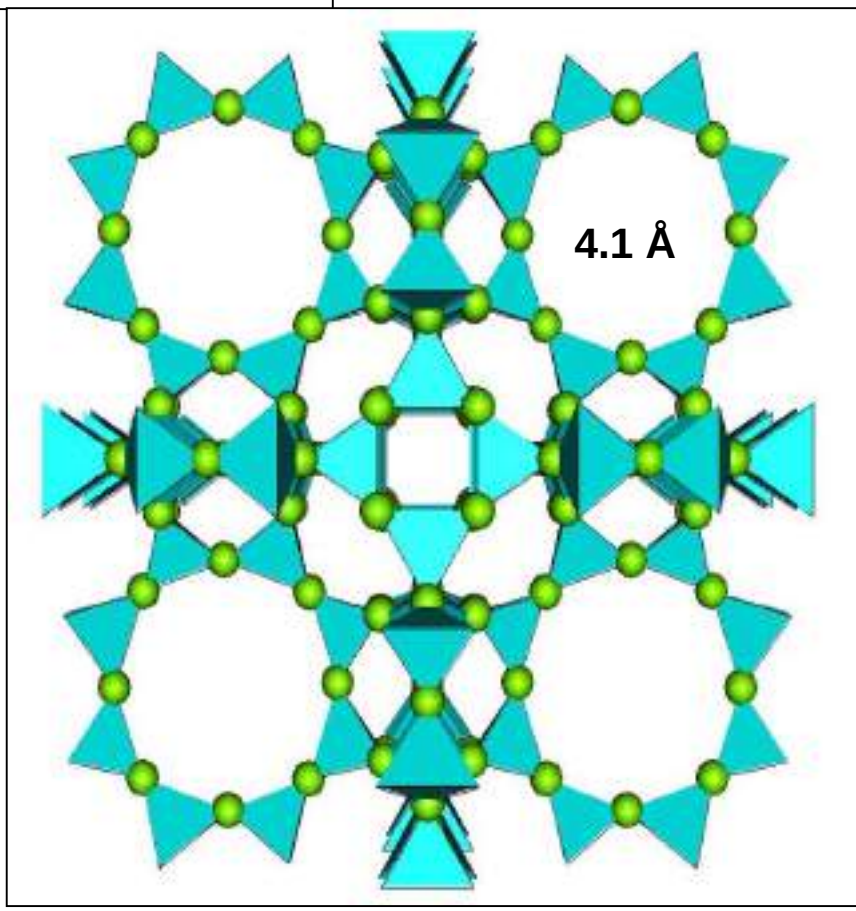

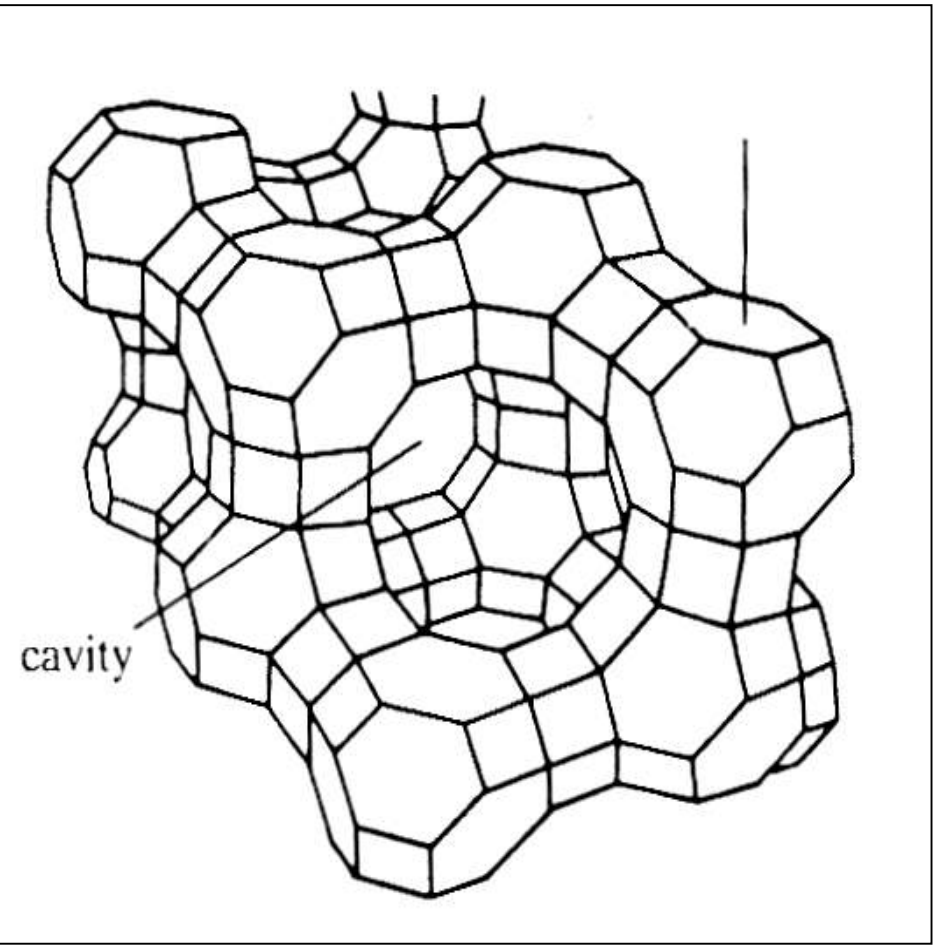

Zeolite Y
(Faujasite)

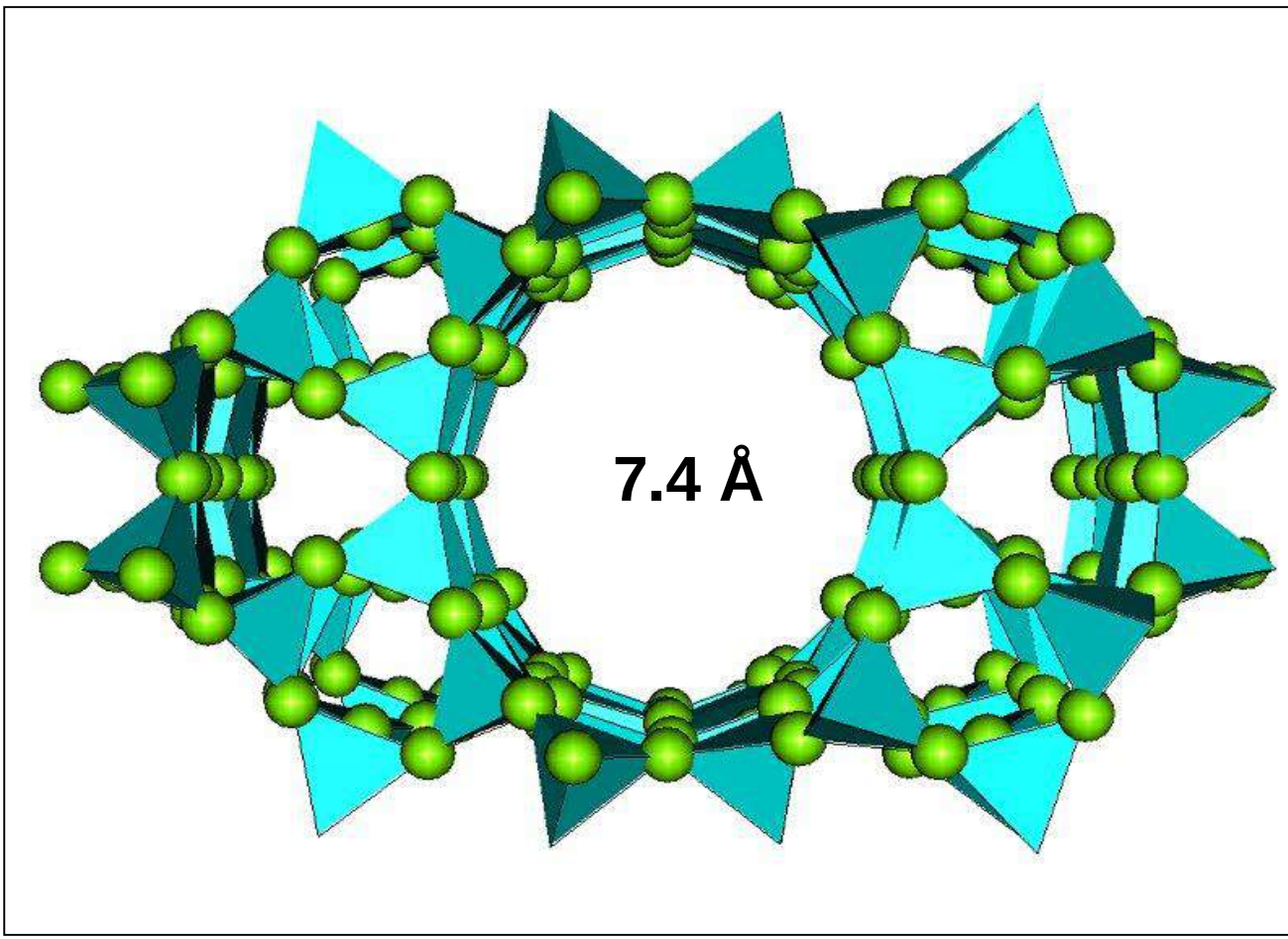

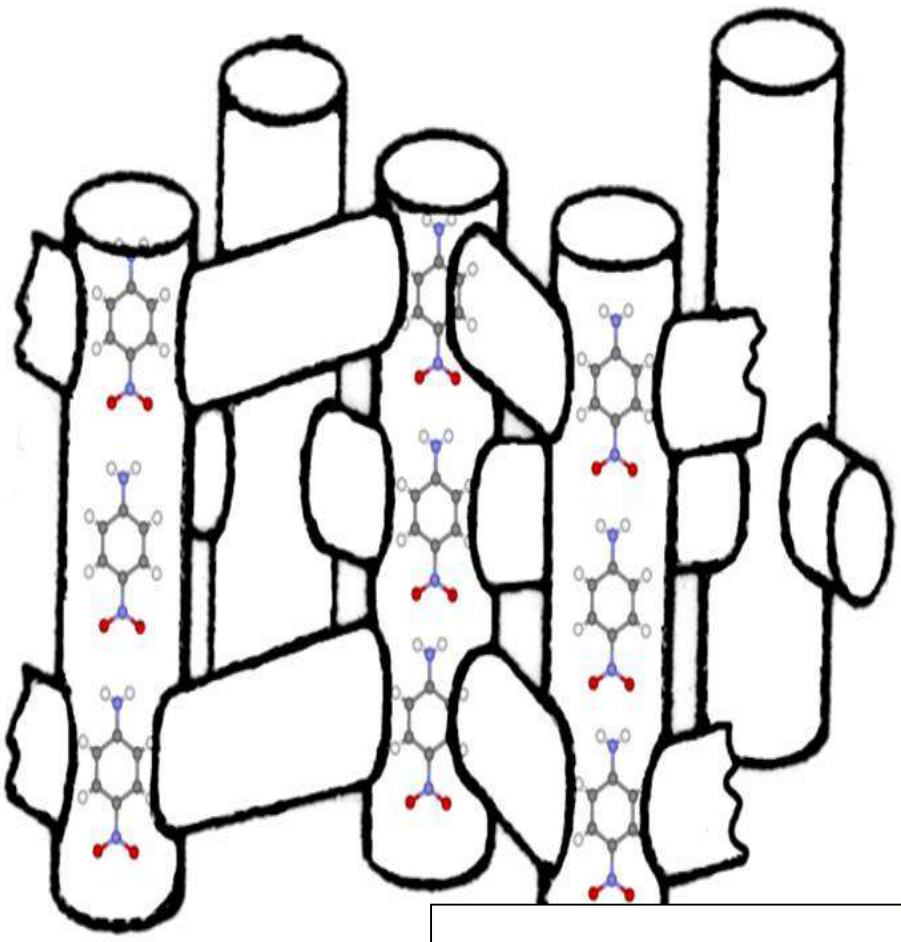

Zeolite ZSM-5

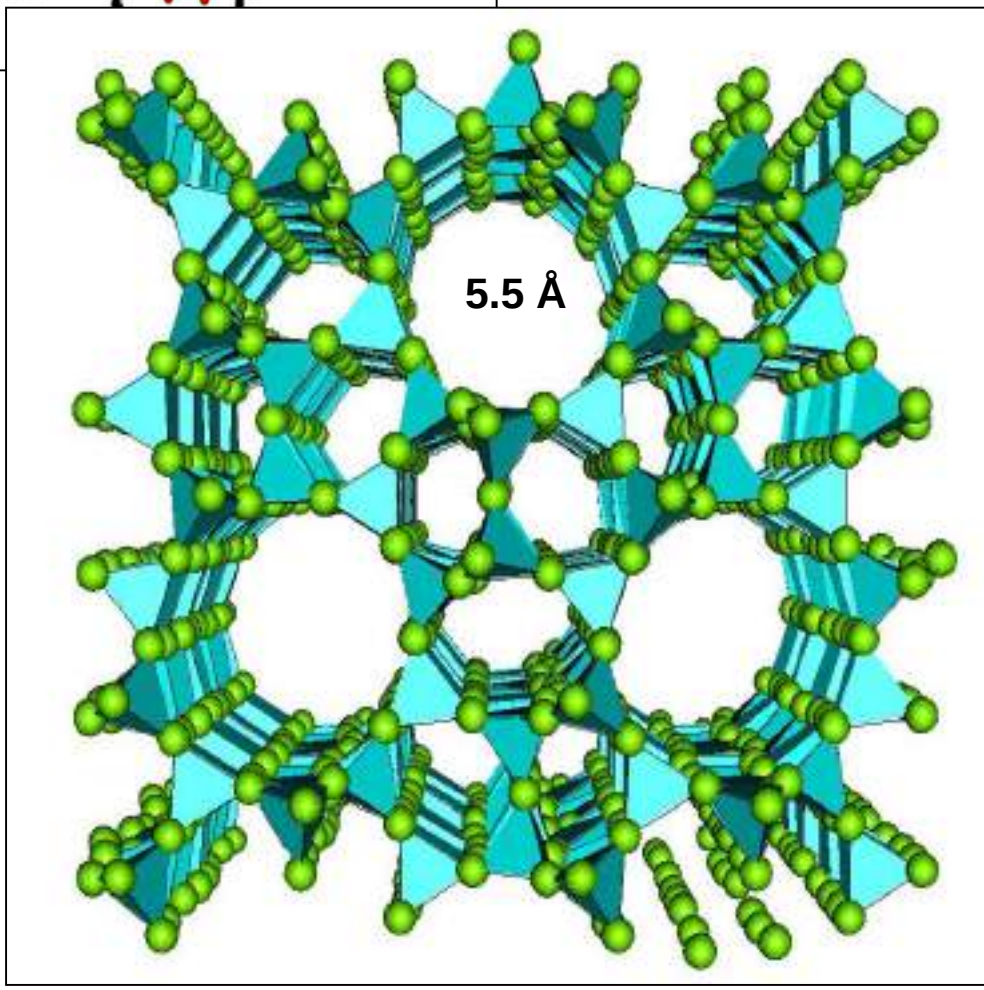

$\delta(^{29}Si)$ in units Q_4(n Al)

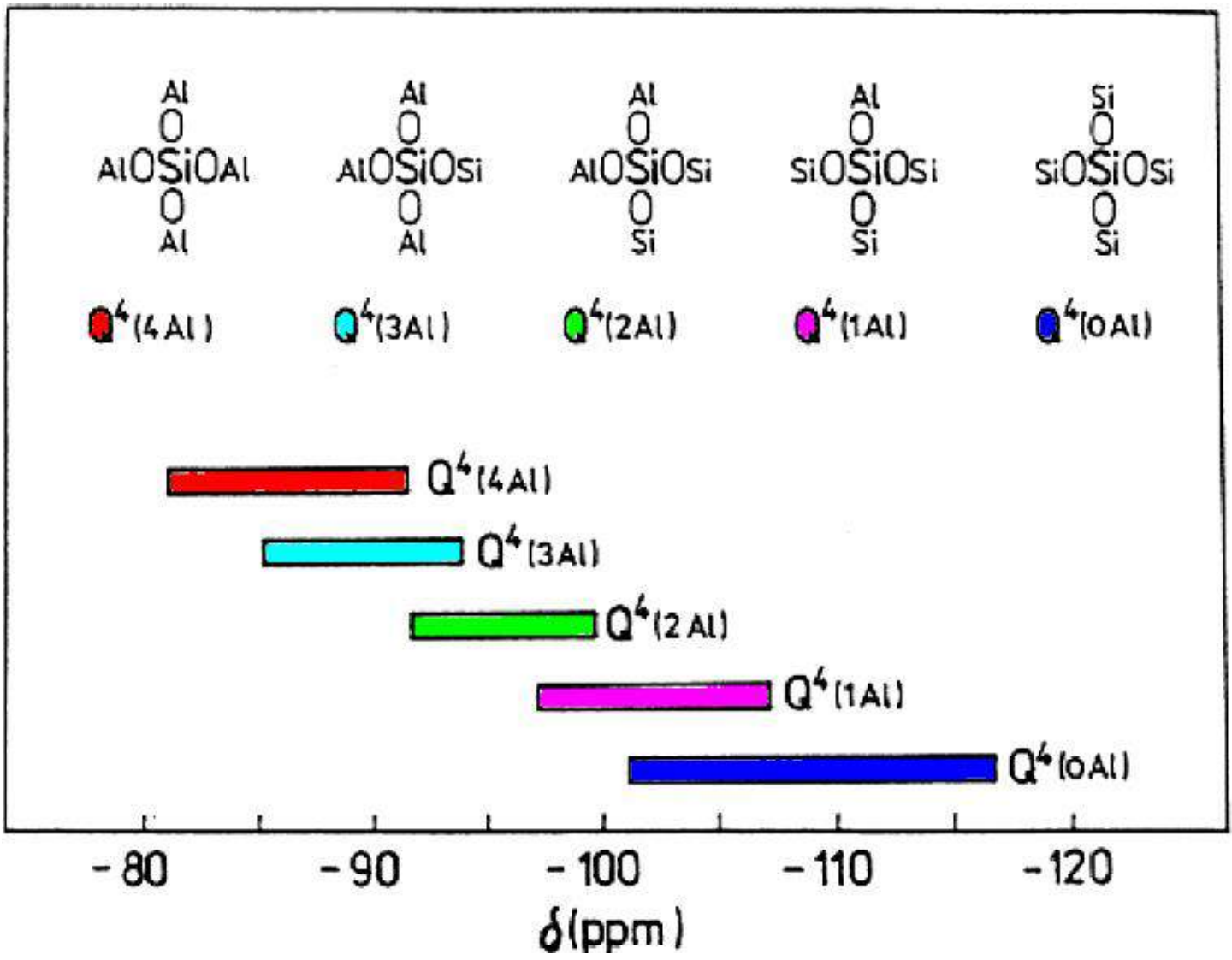

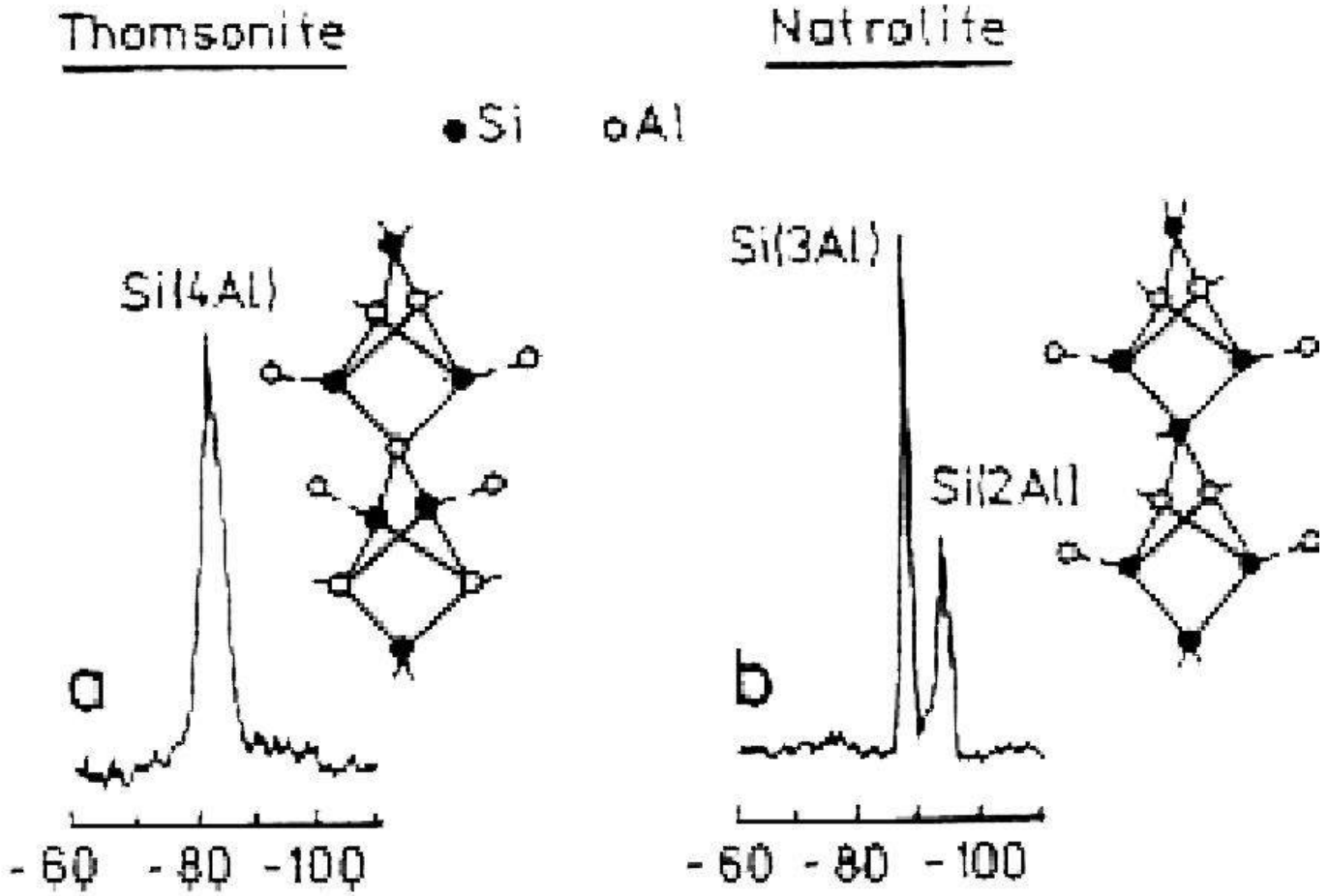
Thomsonite
Natrolite
●Si ○Al
Si(4Al)
Si(3Al)
Si(2Al)
a
b
-60 -80 -100
-60 -80 -100

Variation of ^{29}Si-NMR with Si/Al ratio of faujasite

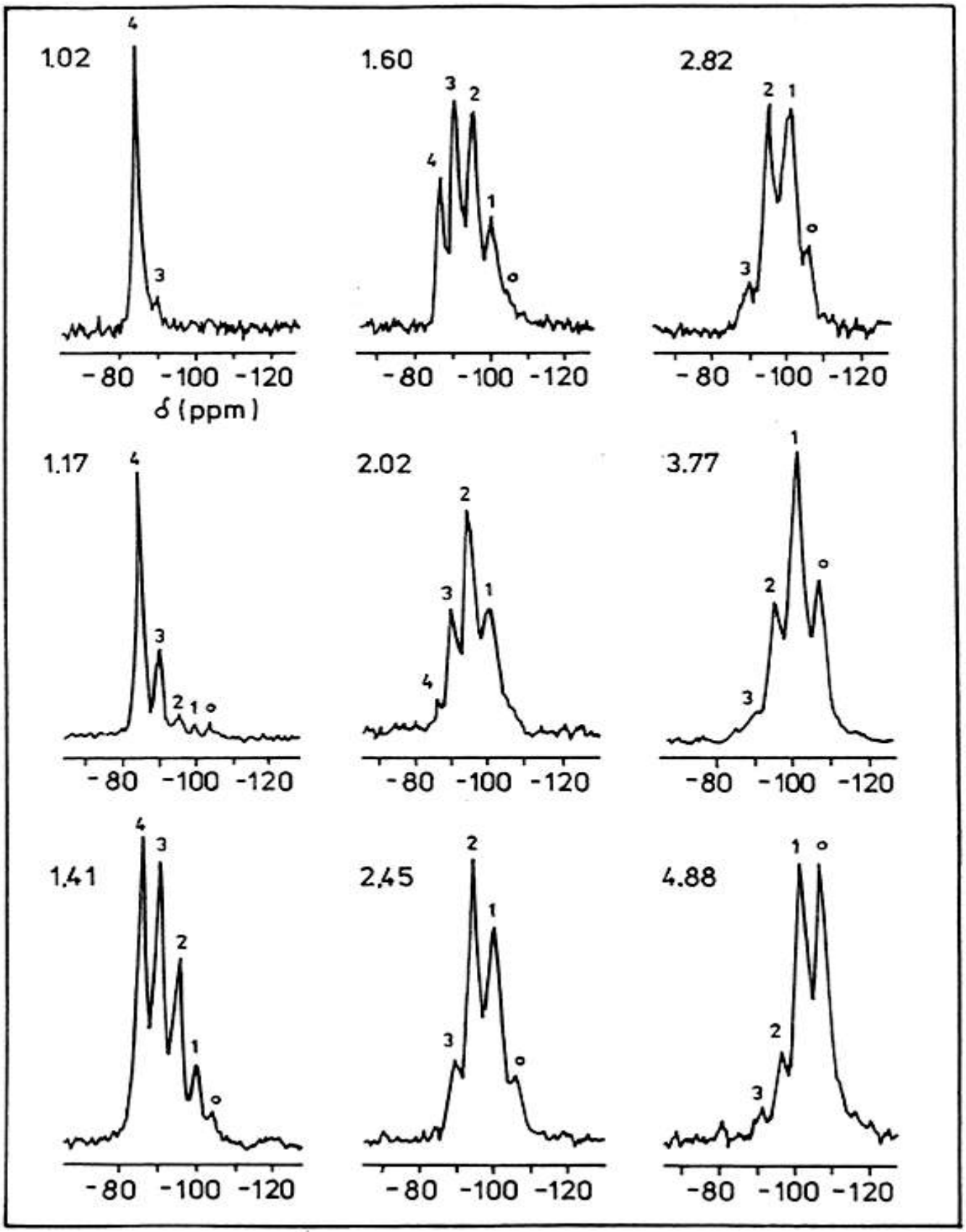

Dealumination of Y zeolite

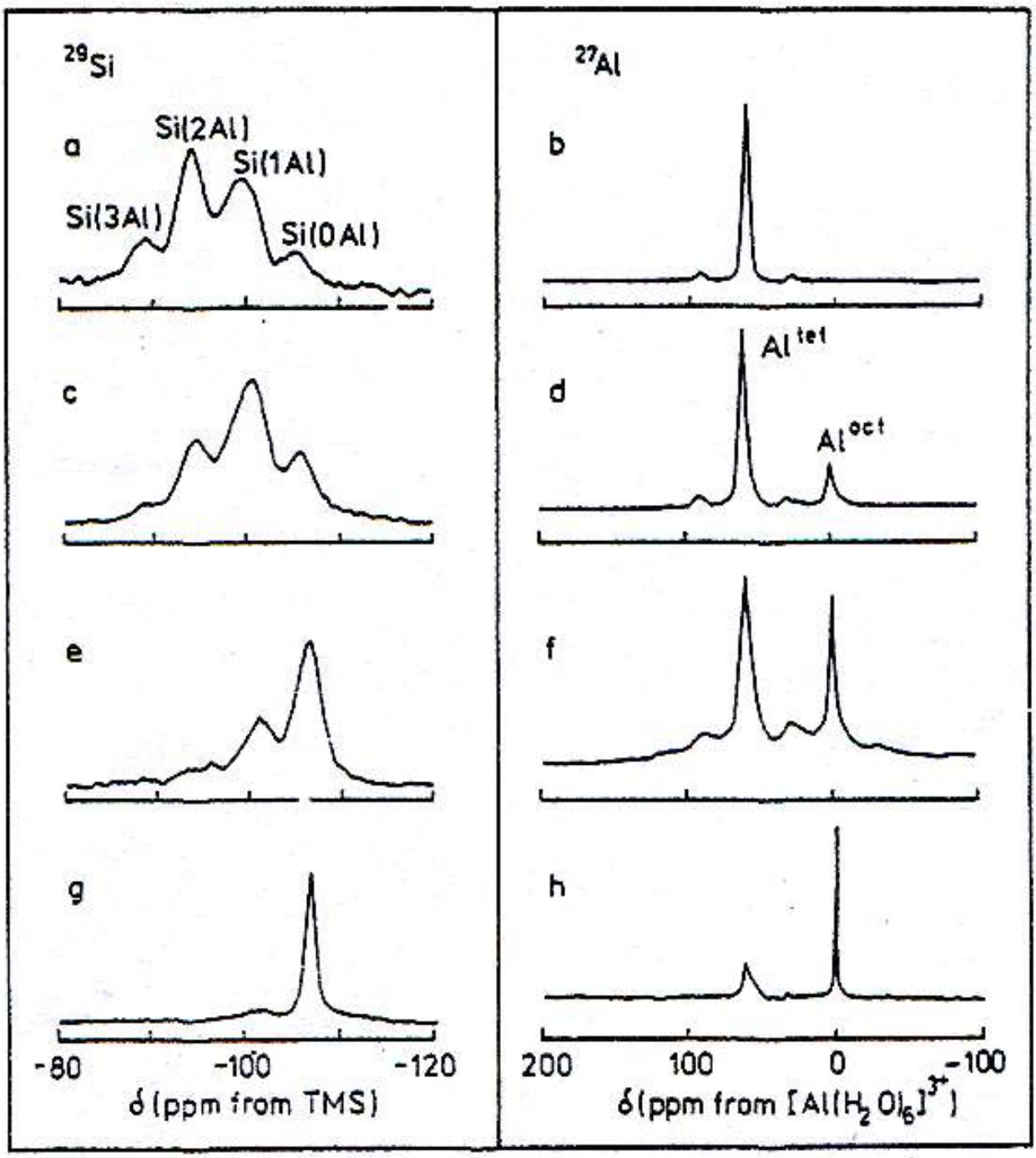

Determination of the ratio Si/Al

$$Si/Al = \sum_{n=0}^{4} I_{Si(nAl)} \Big/ \sum_{n=0}^{4} \frac{n}{4} I_{Si(nAl)}$$

Variation of $\delta(^{29}Si)$ against distance TT

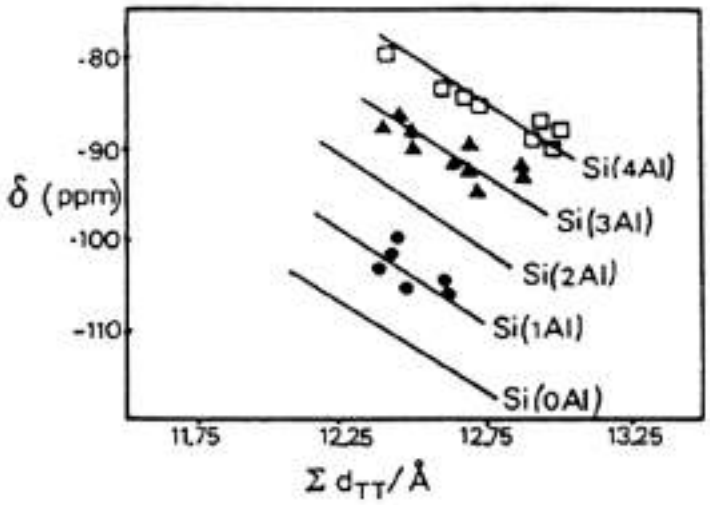

ZSM5. A: static; B: MAS; C: simulation

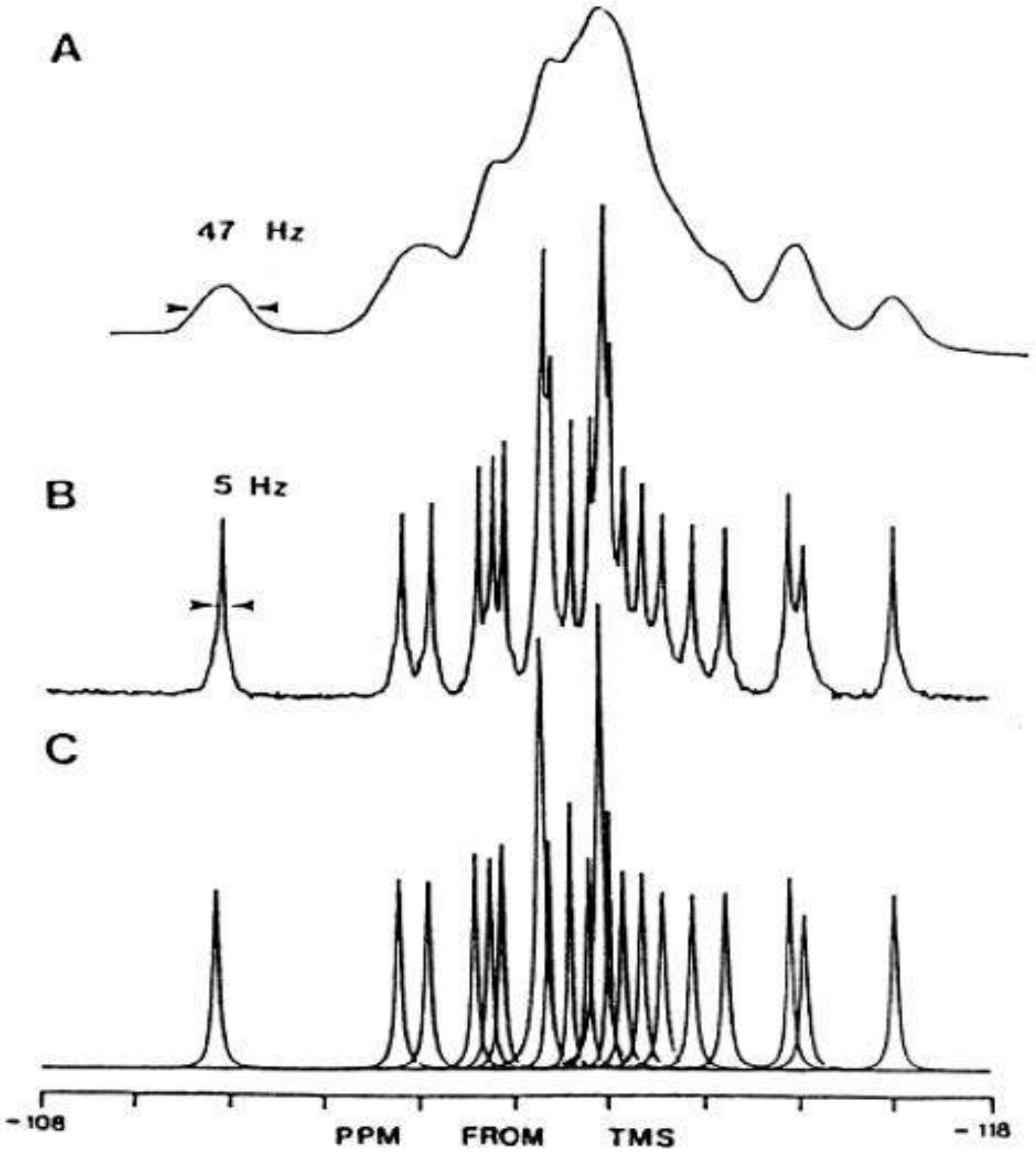

^{29}Si-MAS-NMR of silicalite. Influence of p-xylene concentration.Transformation of monoclinique into orthorhombique symetry

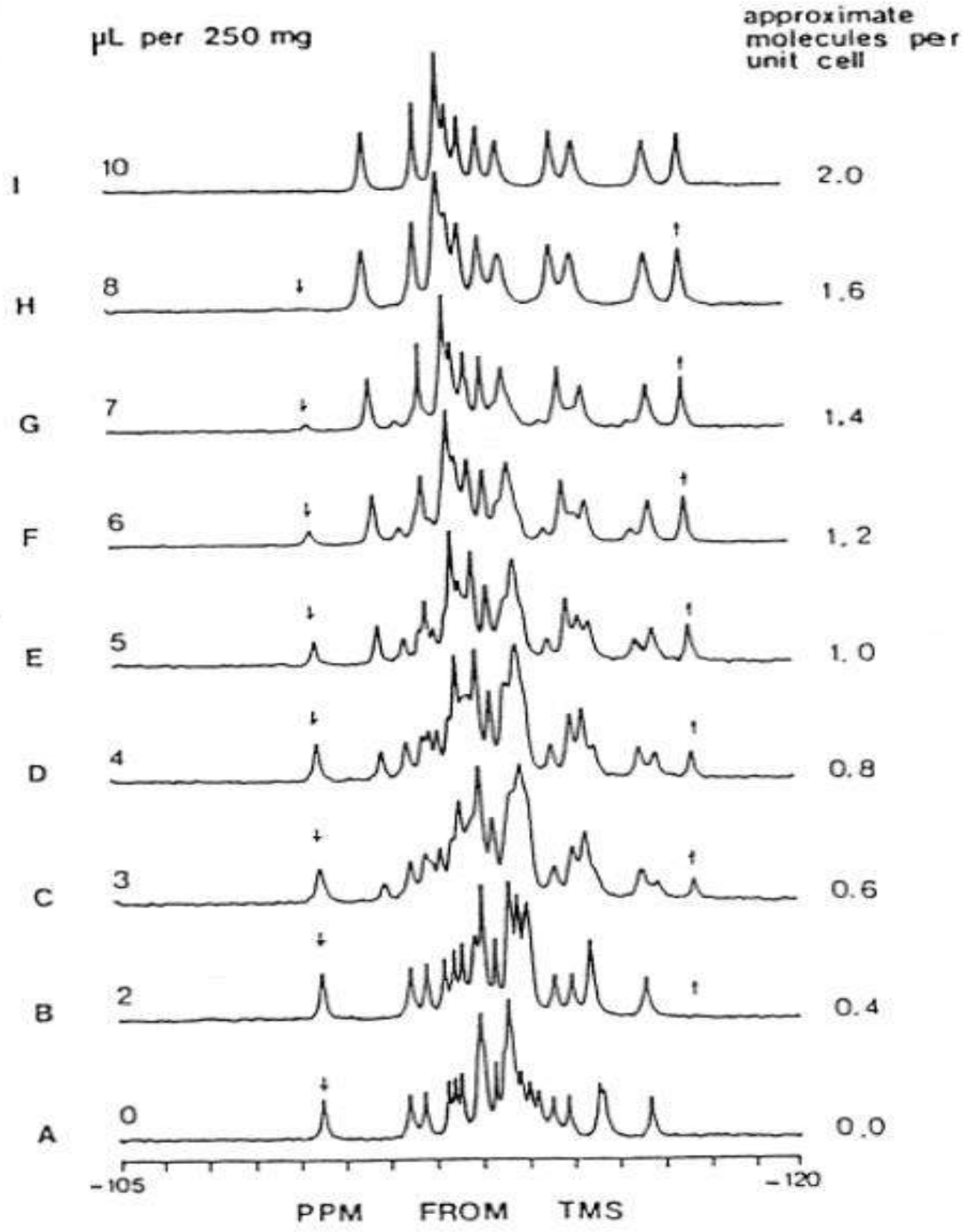

$\delta(^{29}Si)$ during the synthesis of ZSM5 crystallinity: a) 0% Si/Al=1.8 b) 45% Si/Al=5; c) 100%

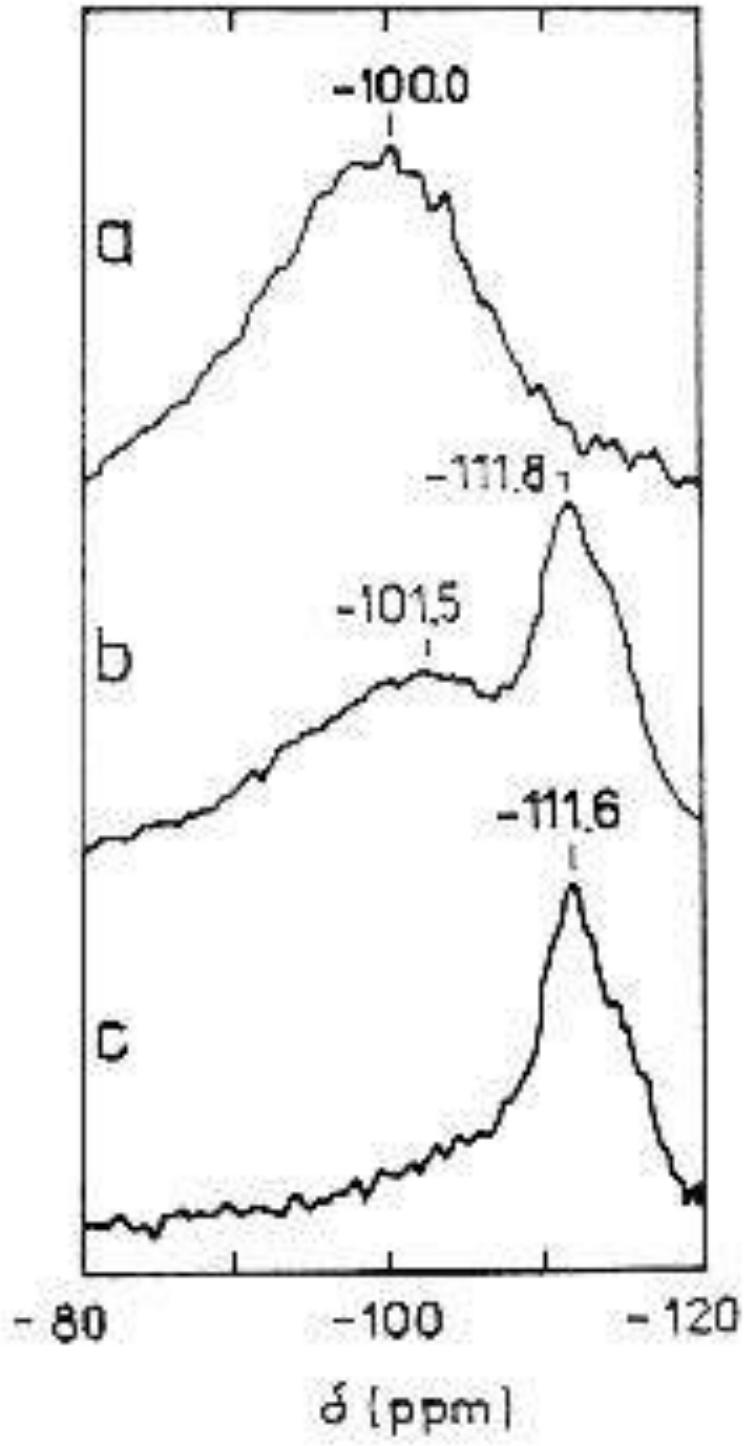

$\delta(^{27}Al)$ of AlO_n

reference $[Al(H2O)_6]^{3+}$

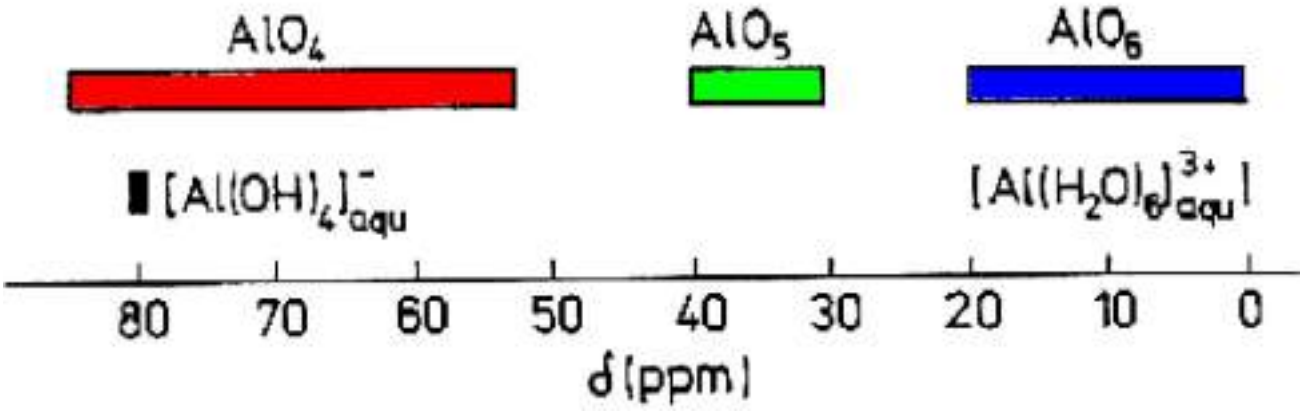

Variation of δ^{27}Al versus Al-O-Si angle

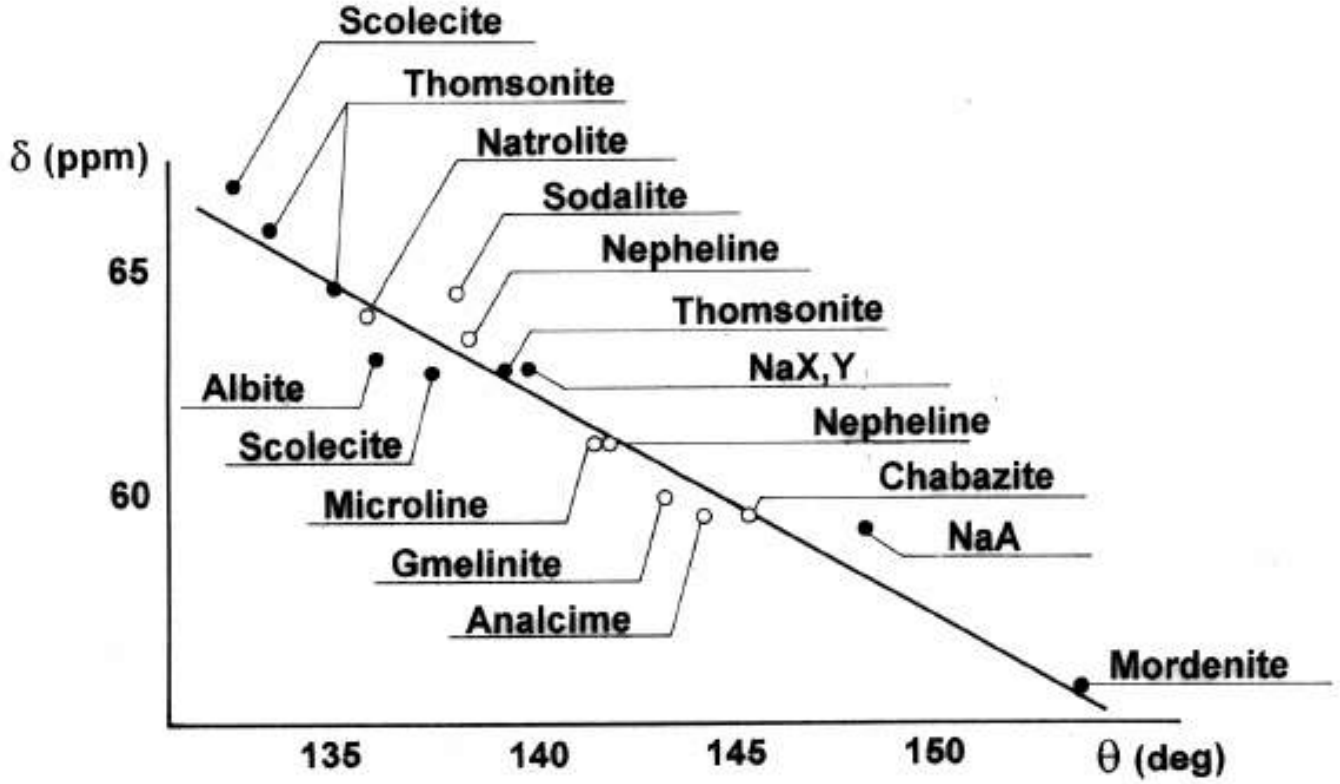

FIG. 3.36 – Variation de $\delta(^{27}Al)$ avec l'angle Al-O-Si.

Spectre de ^{27}Al
a:sans coke; *b:* avec 10 % coke;
*c:*after regeneration under oxygen

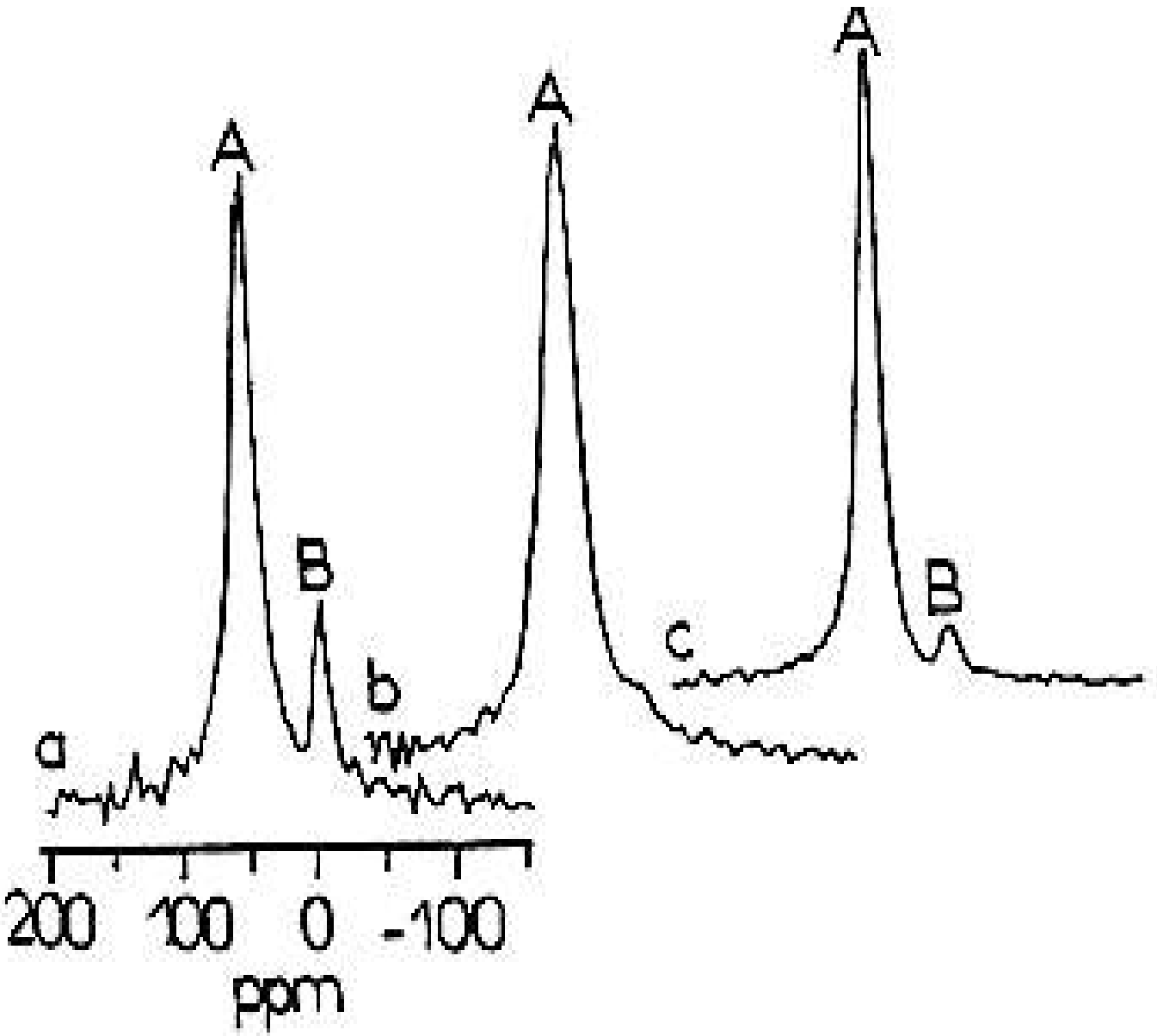

NMR spectroscopy in cement science

Silicon and aluminum coordination

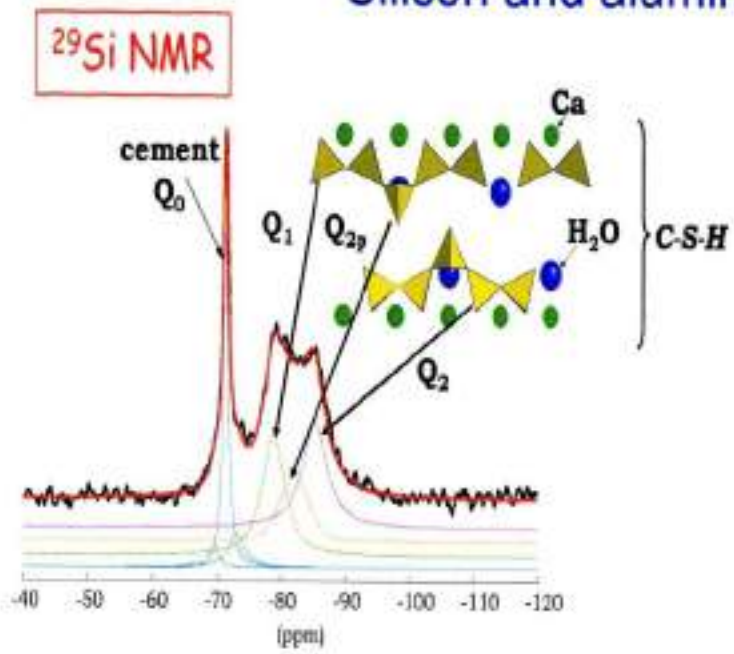

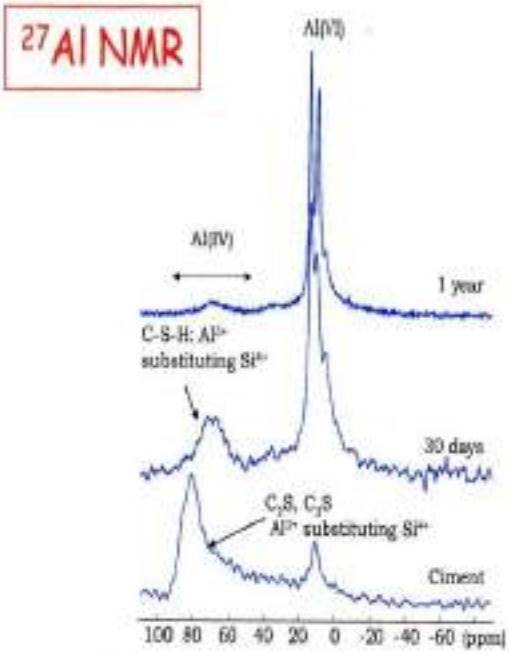

- Solid-state NMR spectroscopy is extensively utilized (^{29}Si, ^{27}Al, ^{1}H):

« Application of NMR spectroscopy to cement science » Gordon and Breach, 1994

« NMR spectroscopy of cement based materials » Springer 1998

- $CaO.SiO_2.Al_2O_3.Fe_2O_3.SO_3.Na_2O.MgO.CO_2.H_2O$
- ^{43}Ca, ^{25}Mg, ^{33}S

Indigo

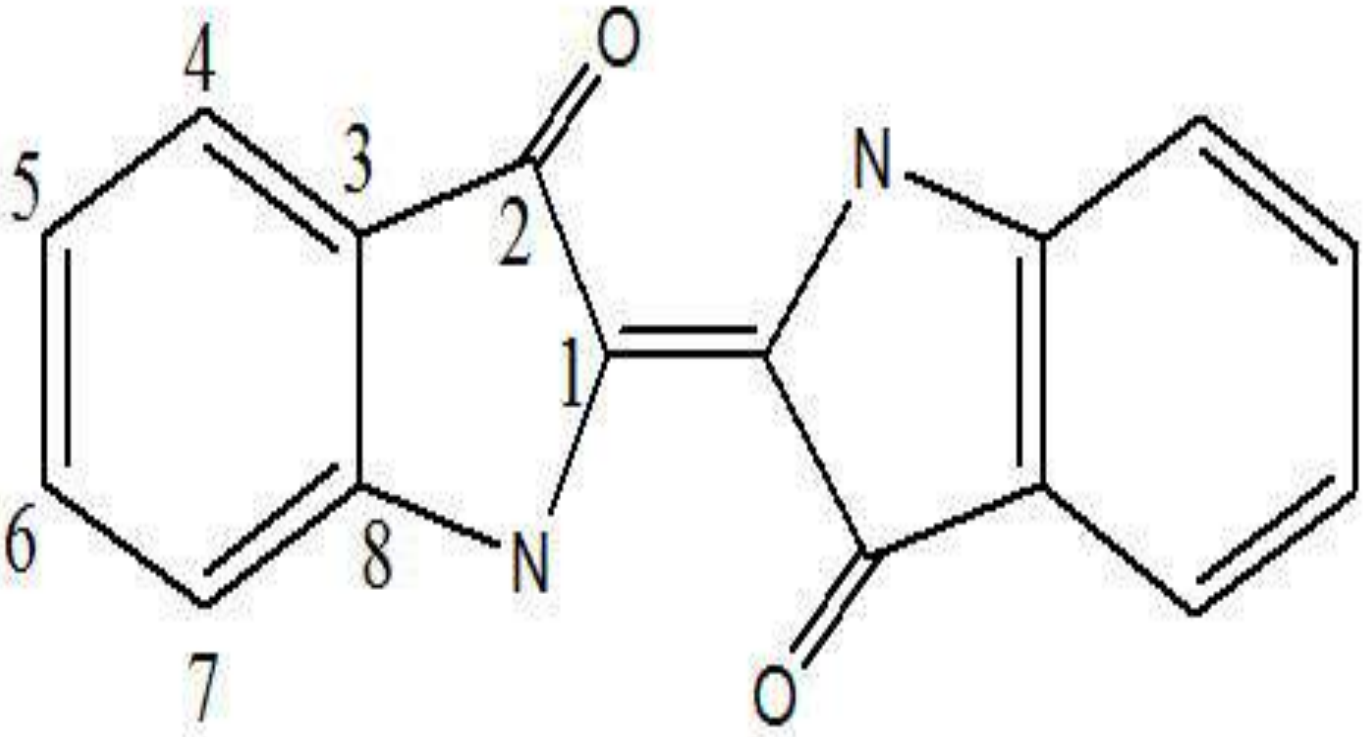

Palygorskite

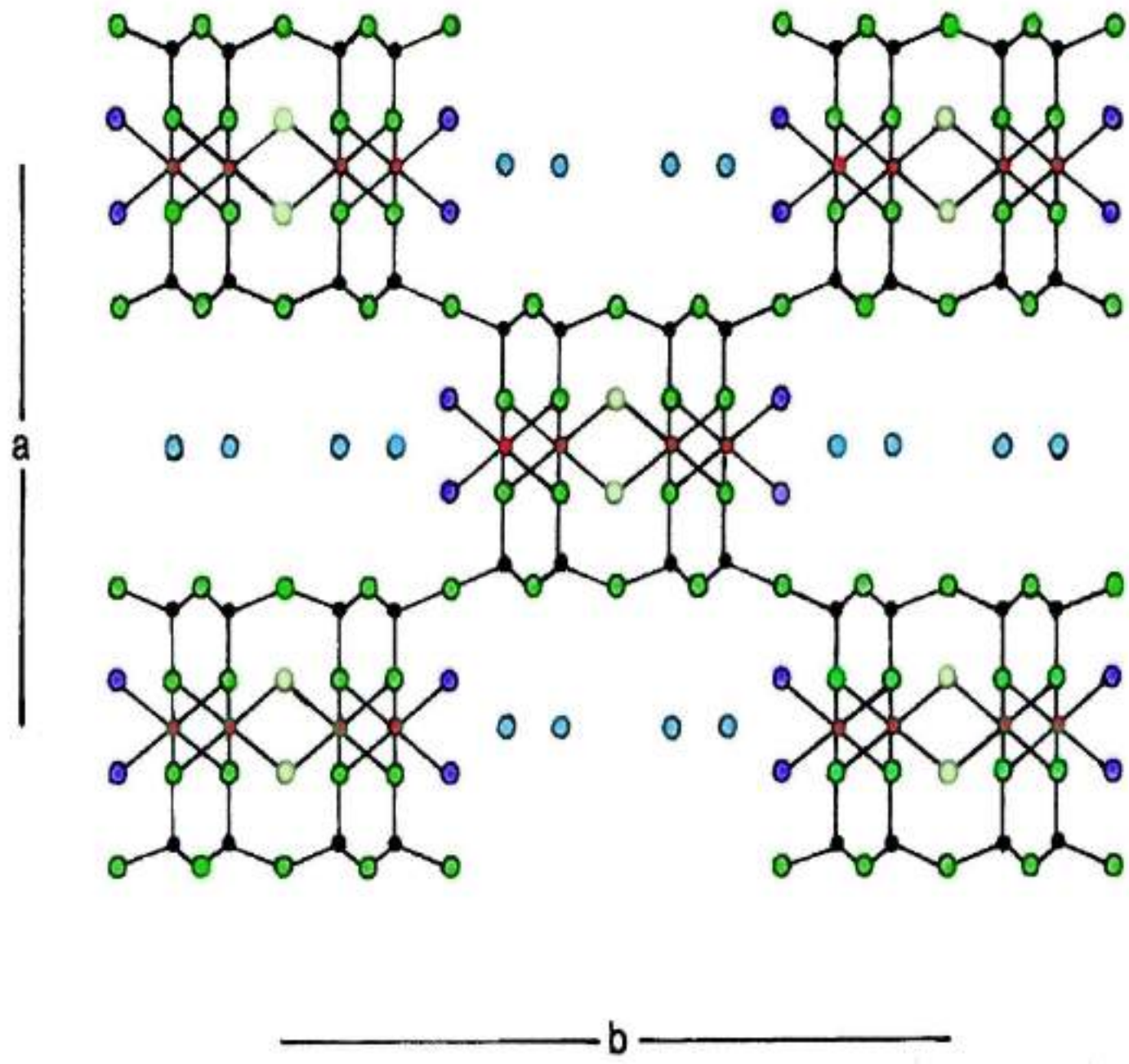

29Si MAS NMR spectra of fresh (a) and aged (b) Maya Bluelike pigments.

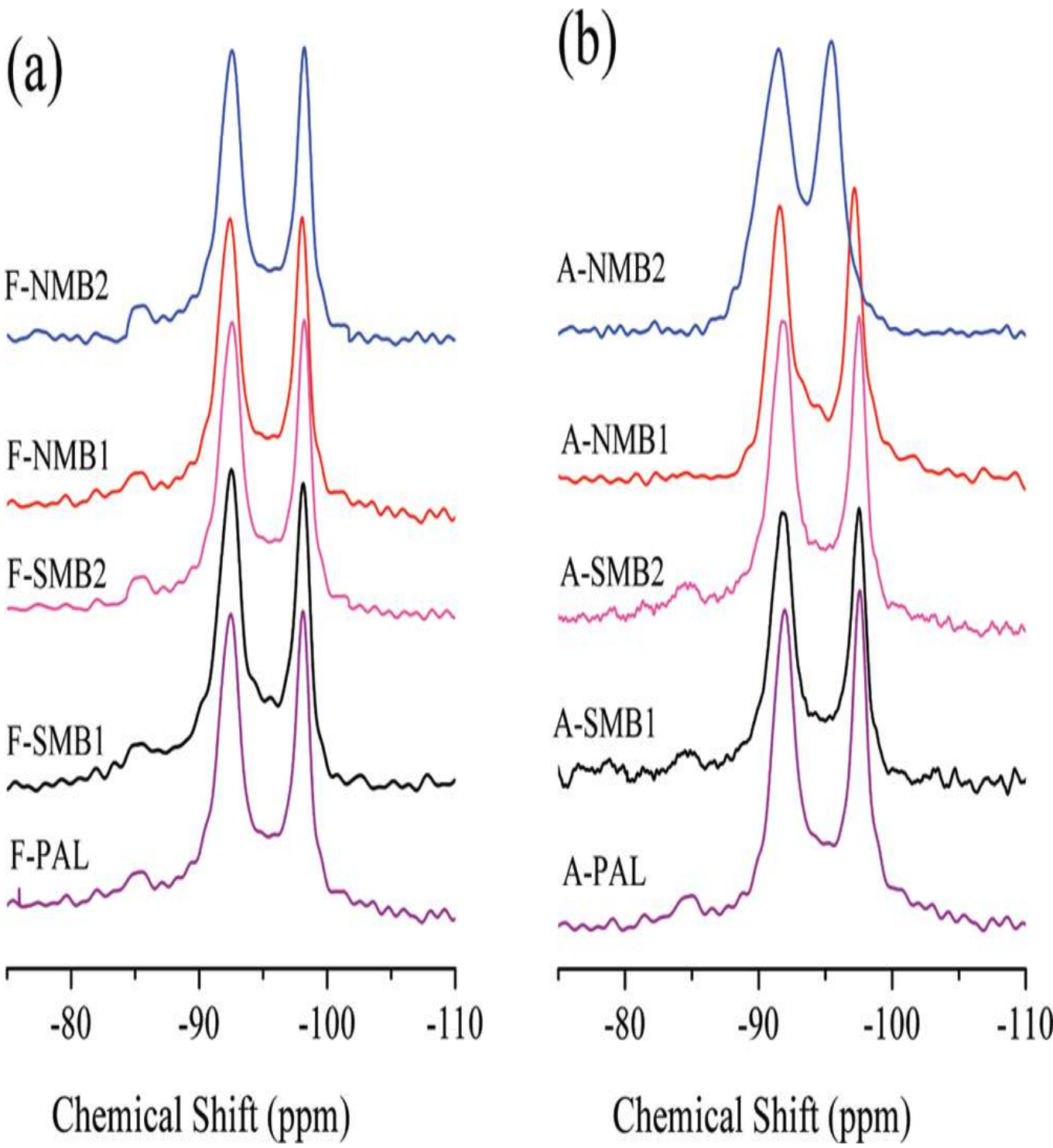

27Al MAS NMR spectra of fresh (a) and aged (b) Maya
Blue-like pigments.

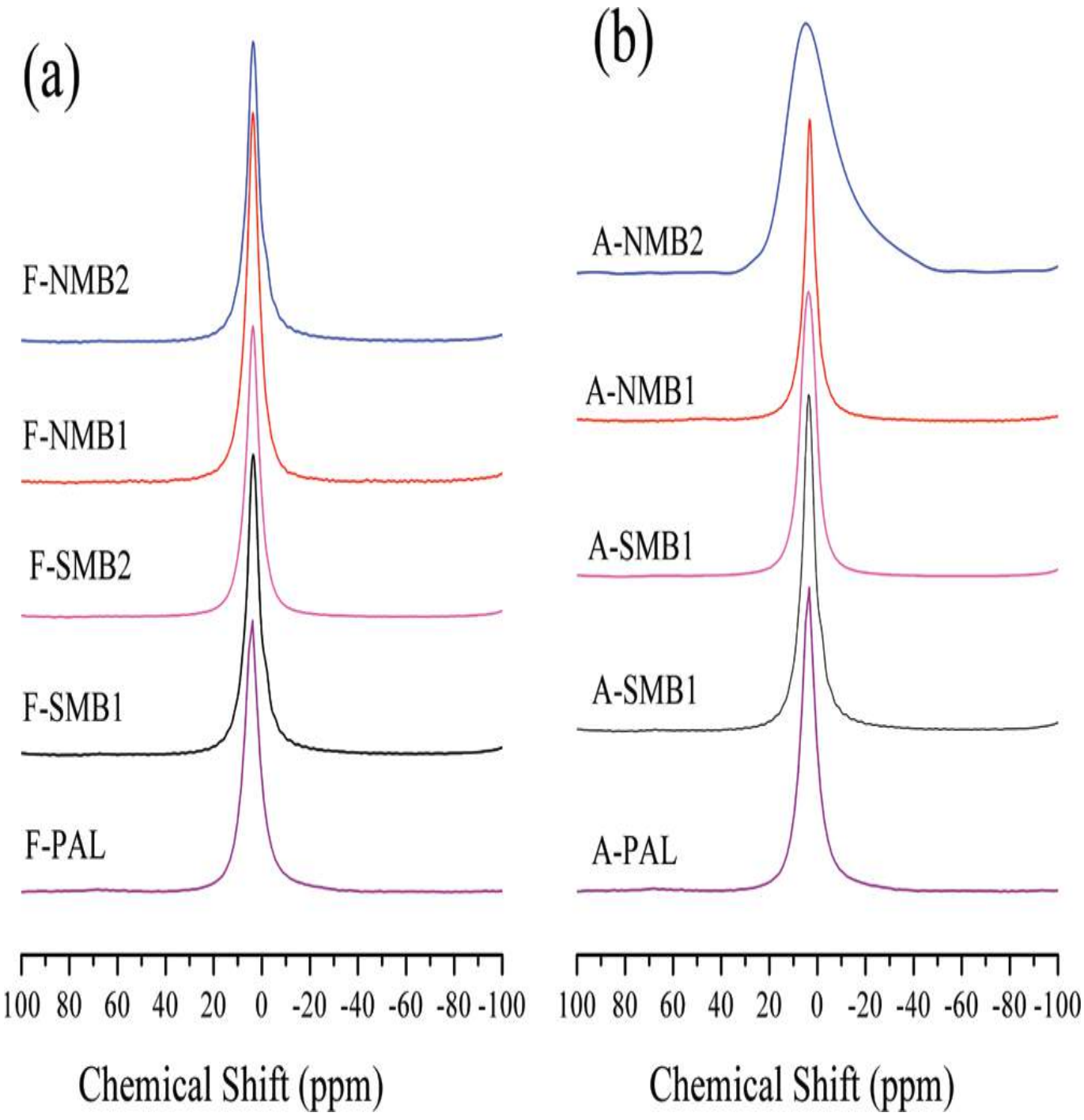

Chemical shift anisotropy

Schematic representation of the ^{13}C NMR absorption of a carbonyl functionality

A- single crystal in two different orientations/B_0

B- In a polycrystalline sample where there are contributions from the random distribution of orientations.

C- In solution

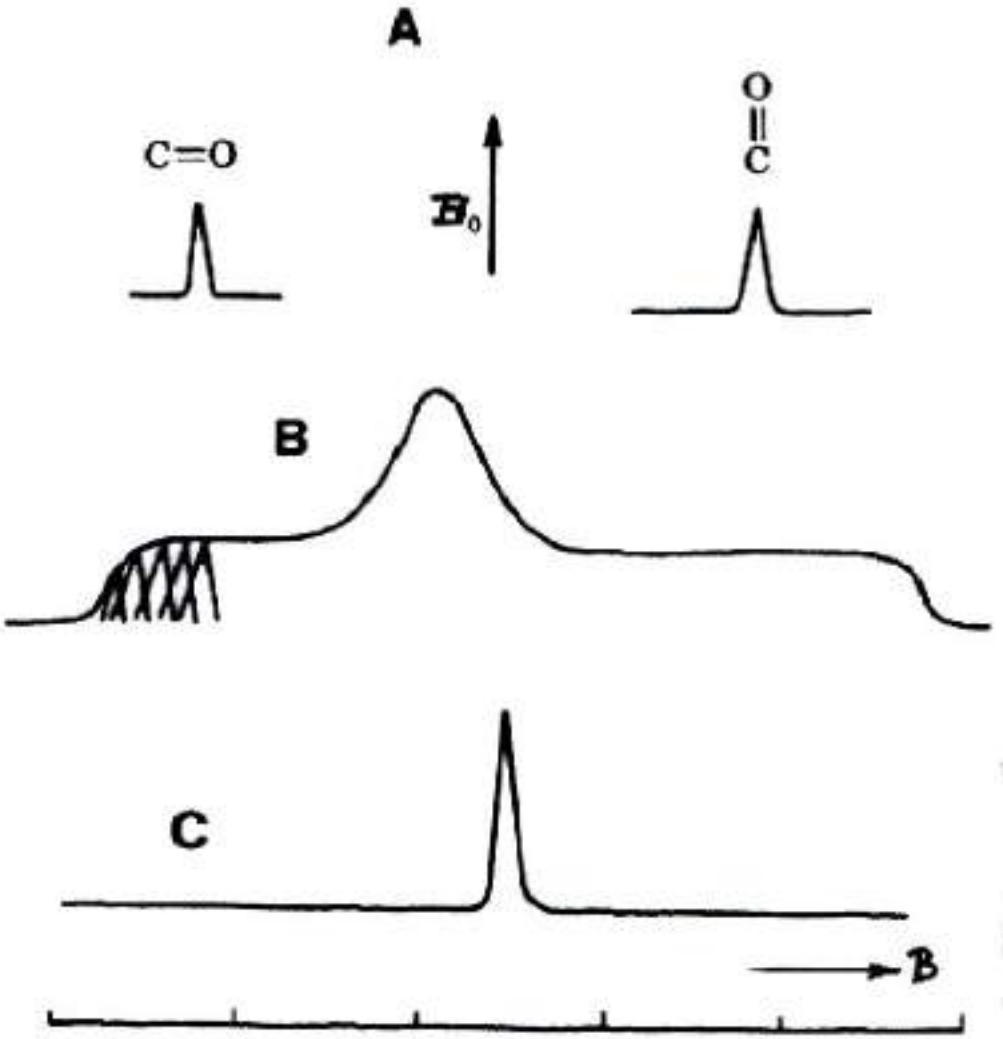

Chemical shift anisotropy

MAS removes all solid-state interactions. Multi-pulse sequence does not remove the chemical shift anisotropy.

Asymmetric shift anisotropy

$$\sigma_{iso} = \sigma_{11} + \sigma_{22} + \sigma_{33}$$

Axially shift anisotropy

$$\sigma_{11} = \sigma_{22} = \sigma_{\perp} \quad \sigma_{33} = \sigma_{II}$$

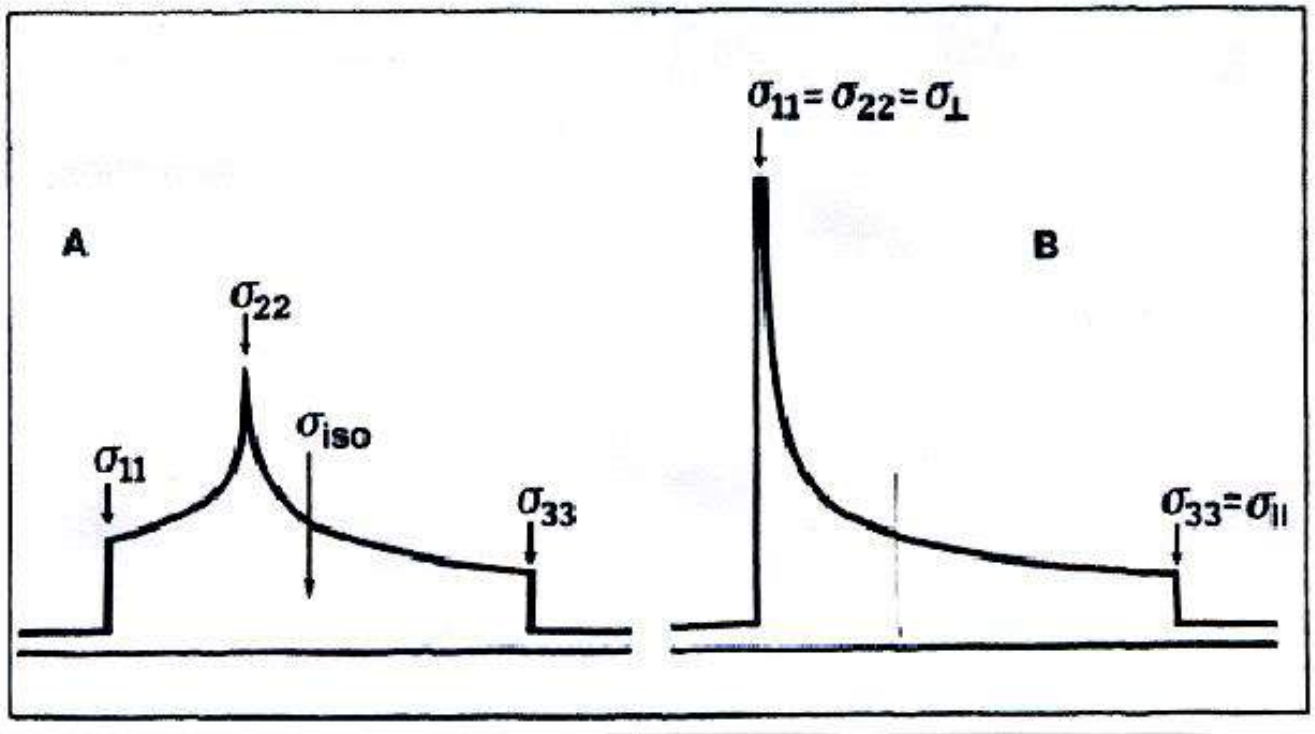

13C spectra of polycrystalline compounds containing carbonyl groups. Low-field: CO; high field: CH3

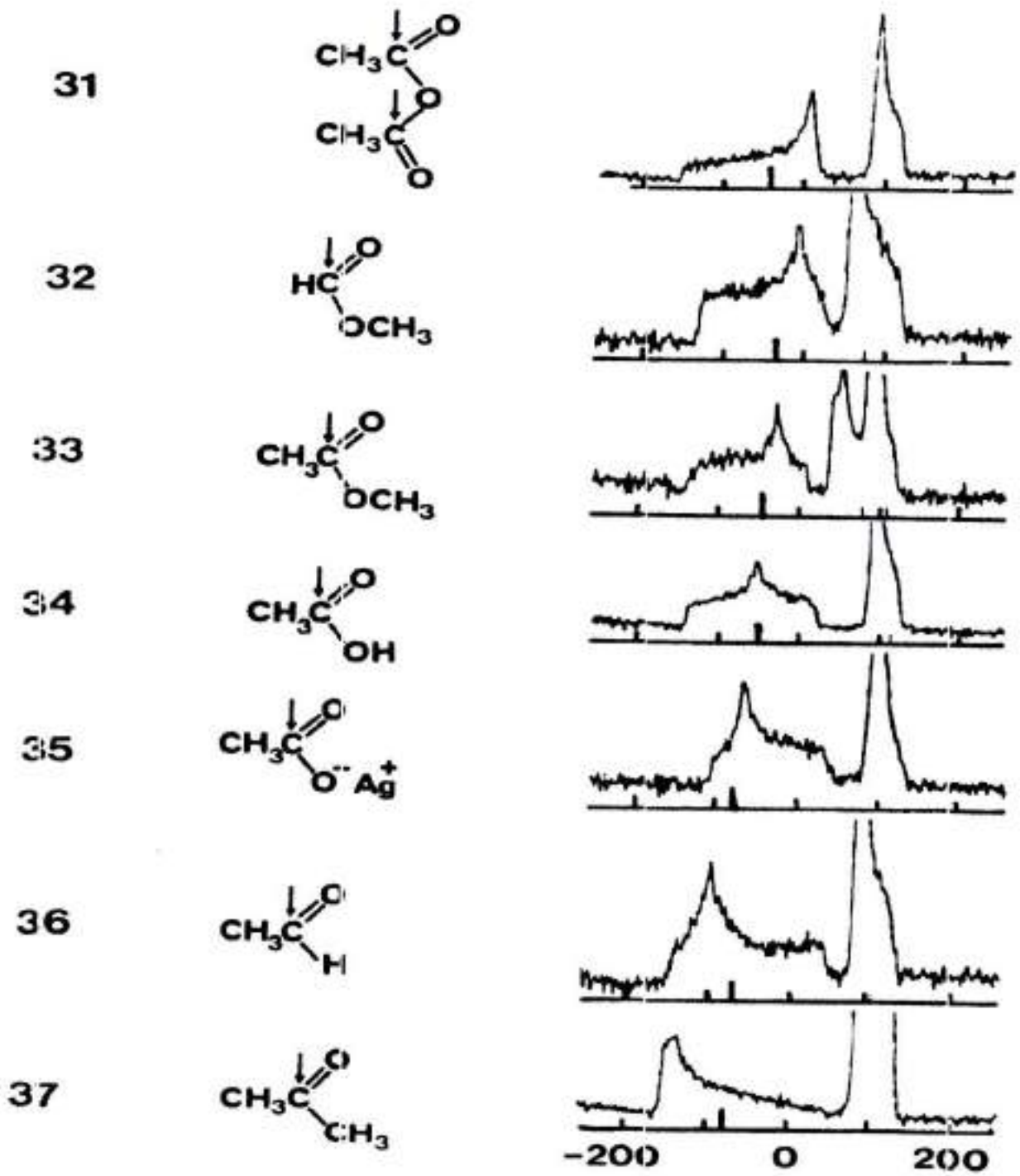

^{31}P NMR

P_4O_6

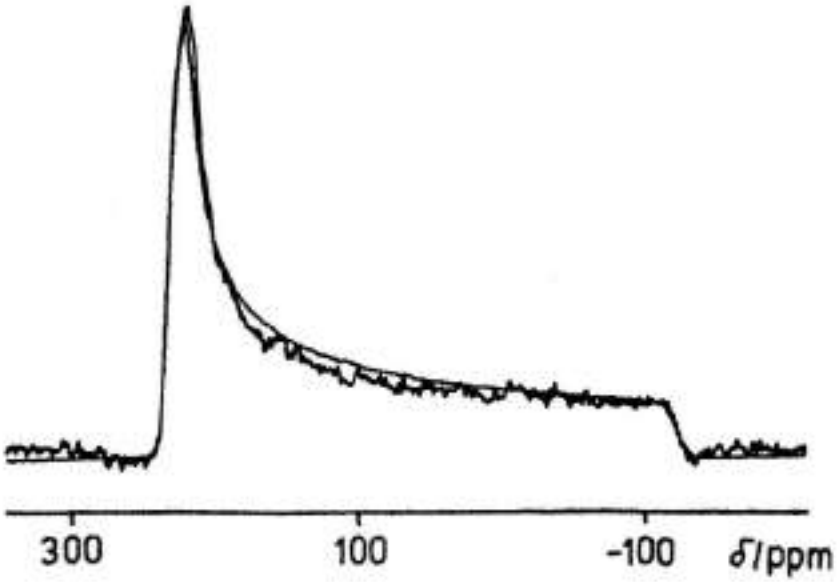

$Ba(Et)_2PO_4$

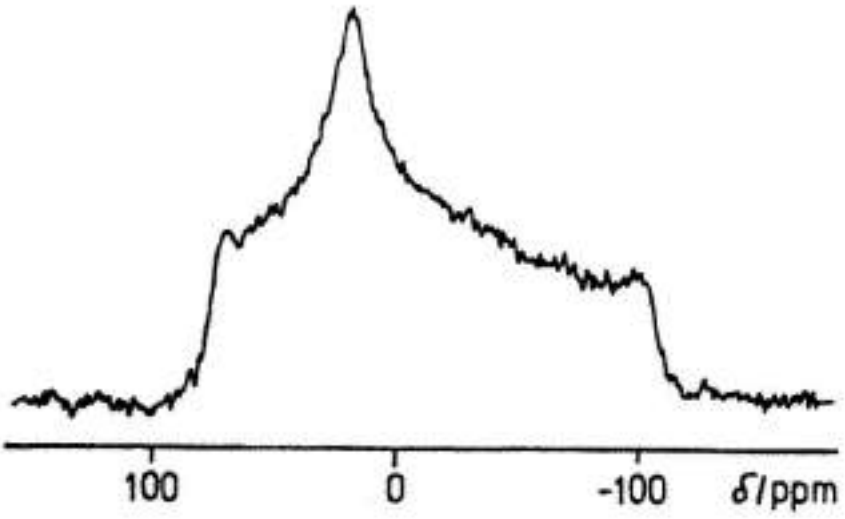

SAPO 11; AlPO11

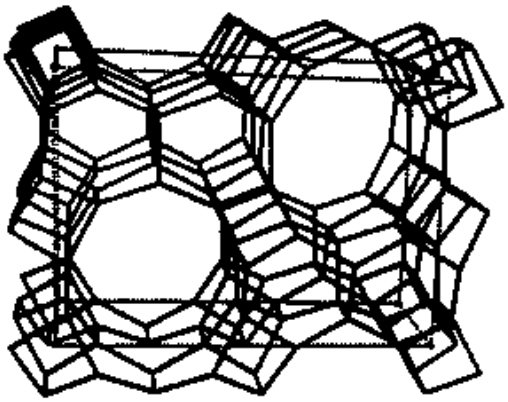

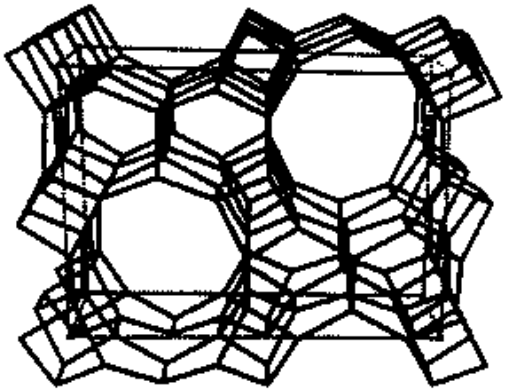

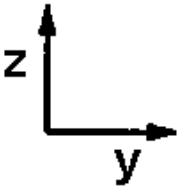

Framework viewed along [100]

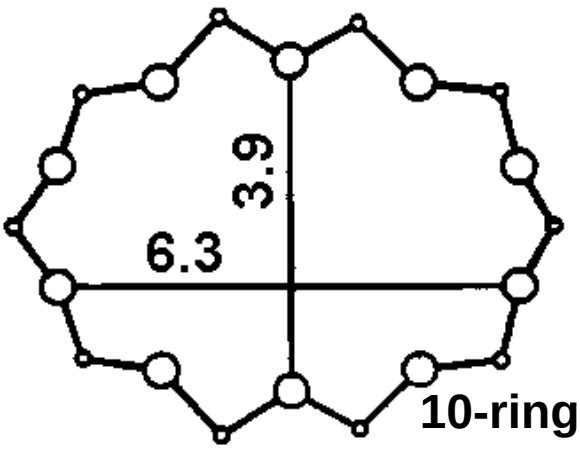

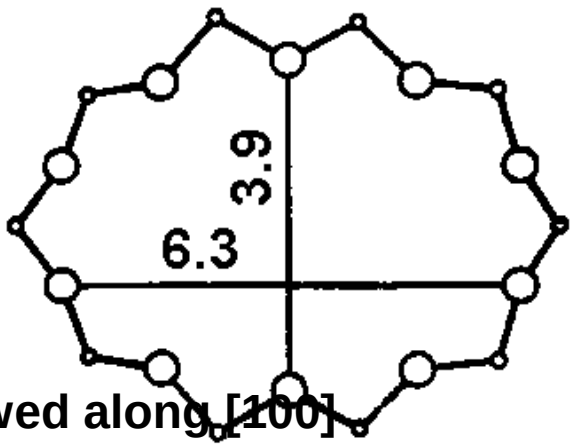

10-ring viewed along [100]

Anisotropy of chemical shift

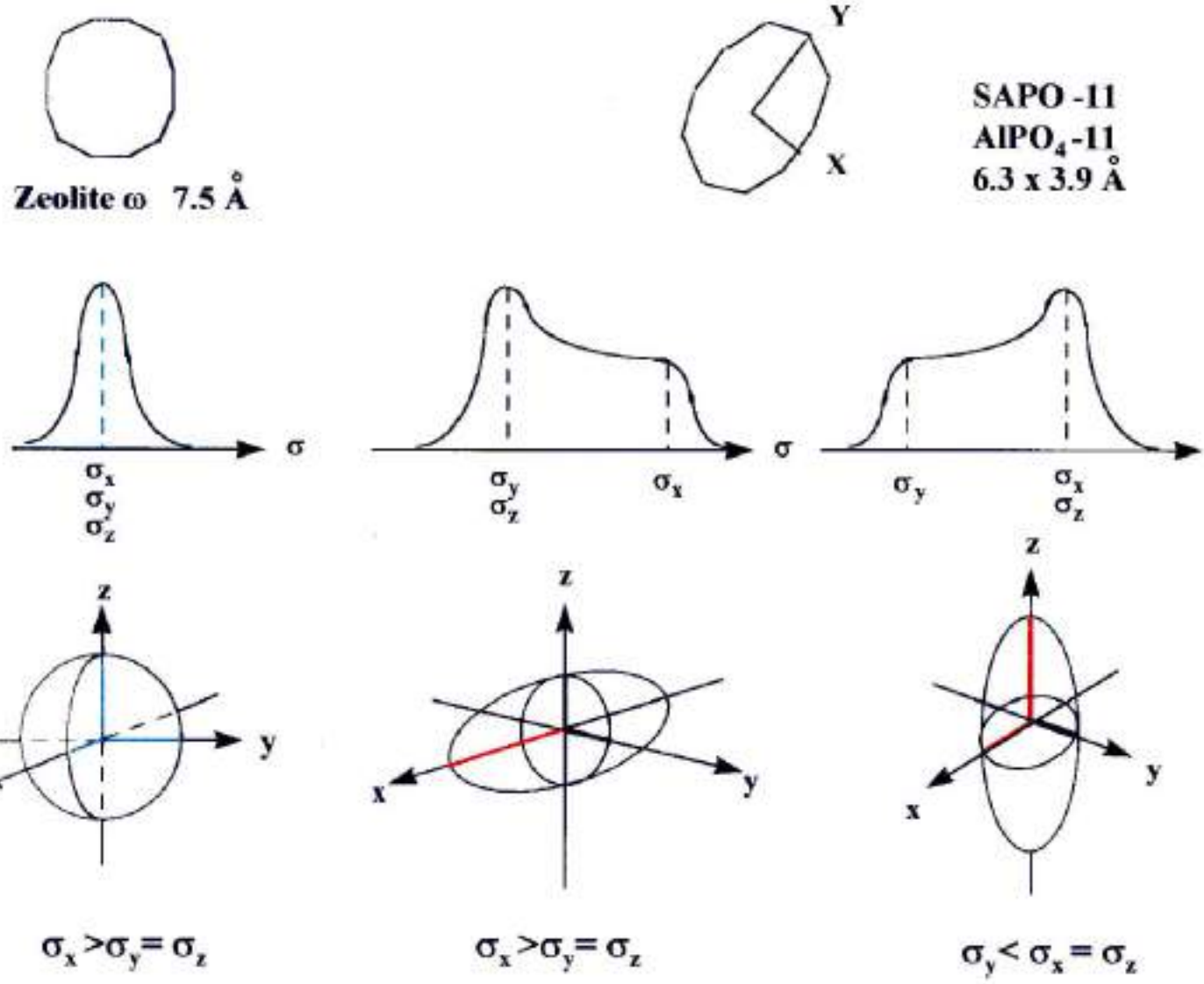

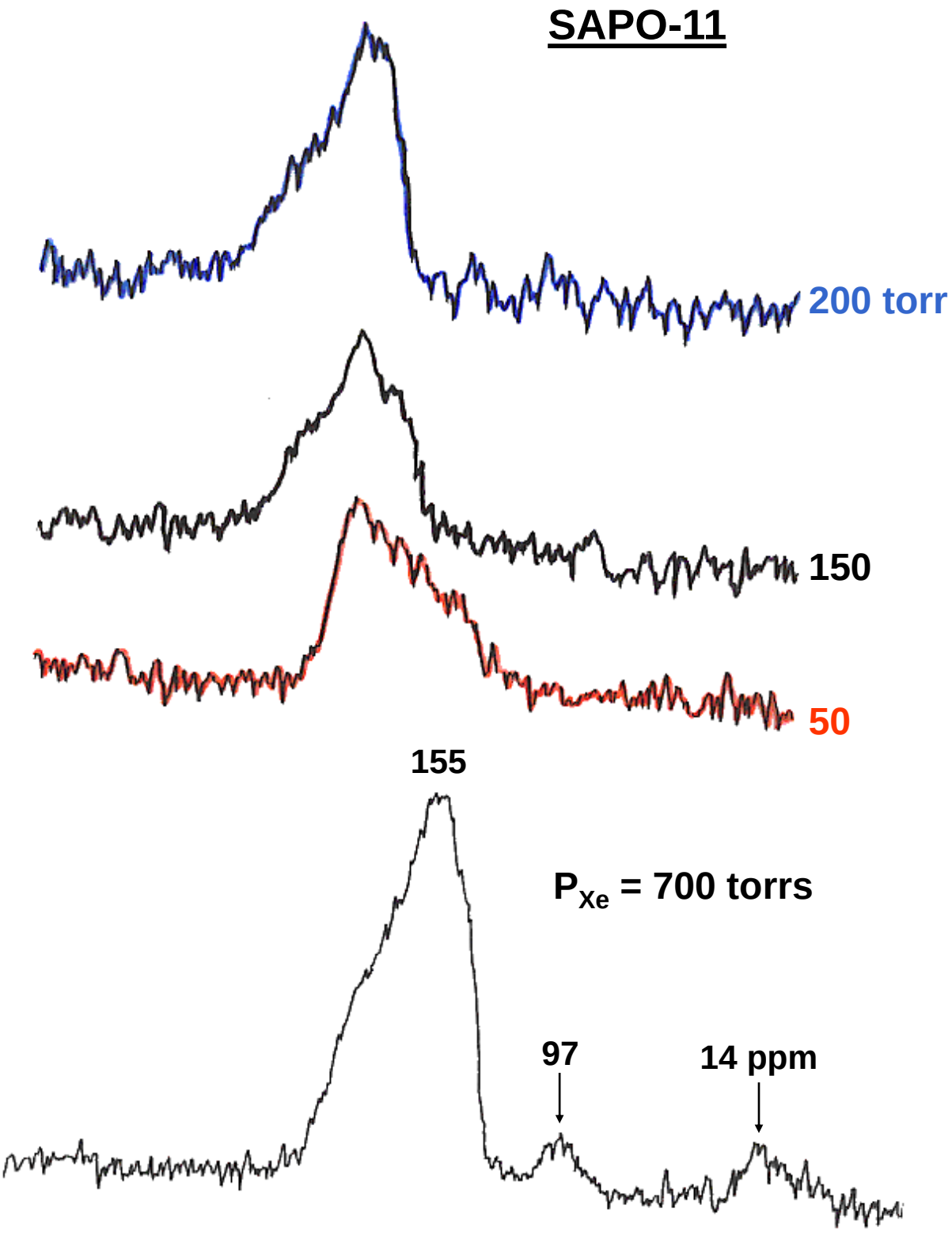

SAPO 11-3

Accuracy of the angle

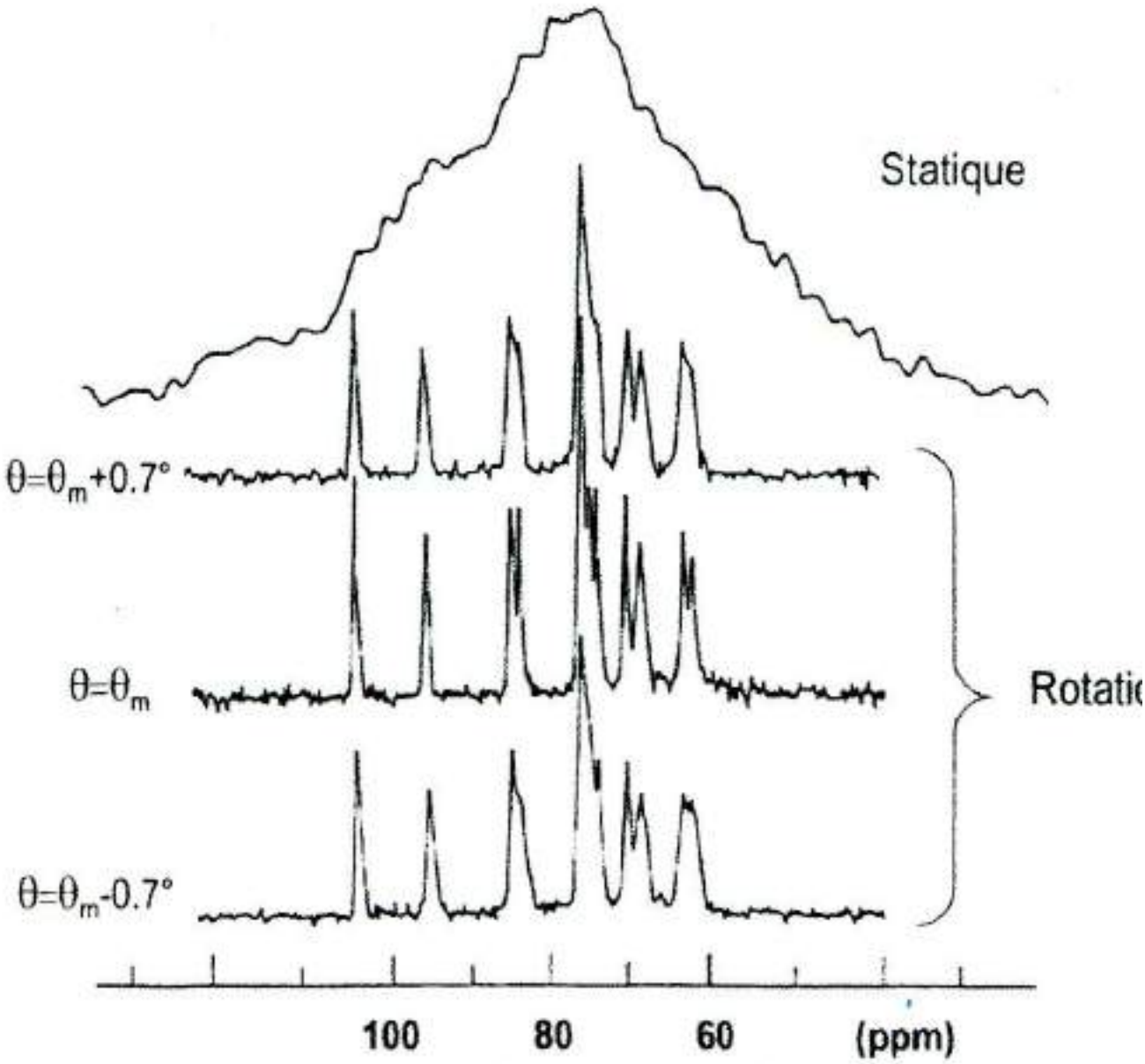

Influence of the rotation on the sidebands

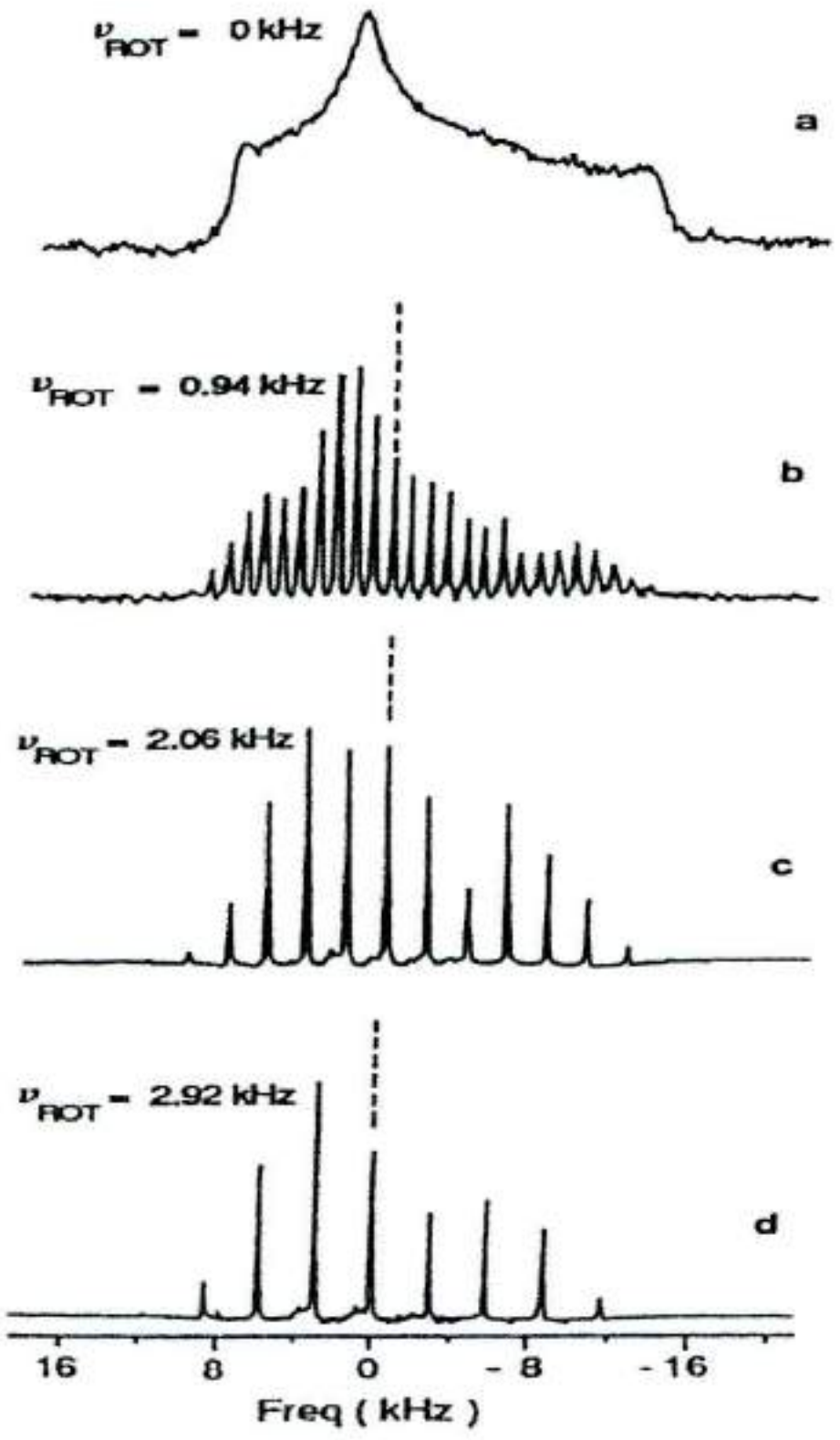

Pyramids and Limestones

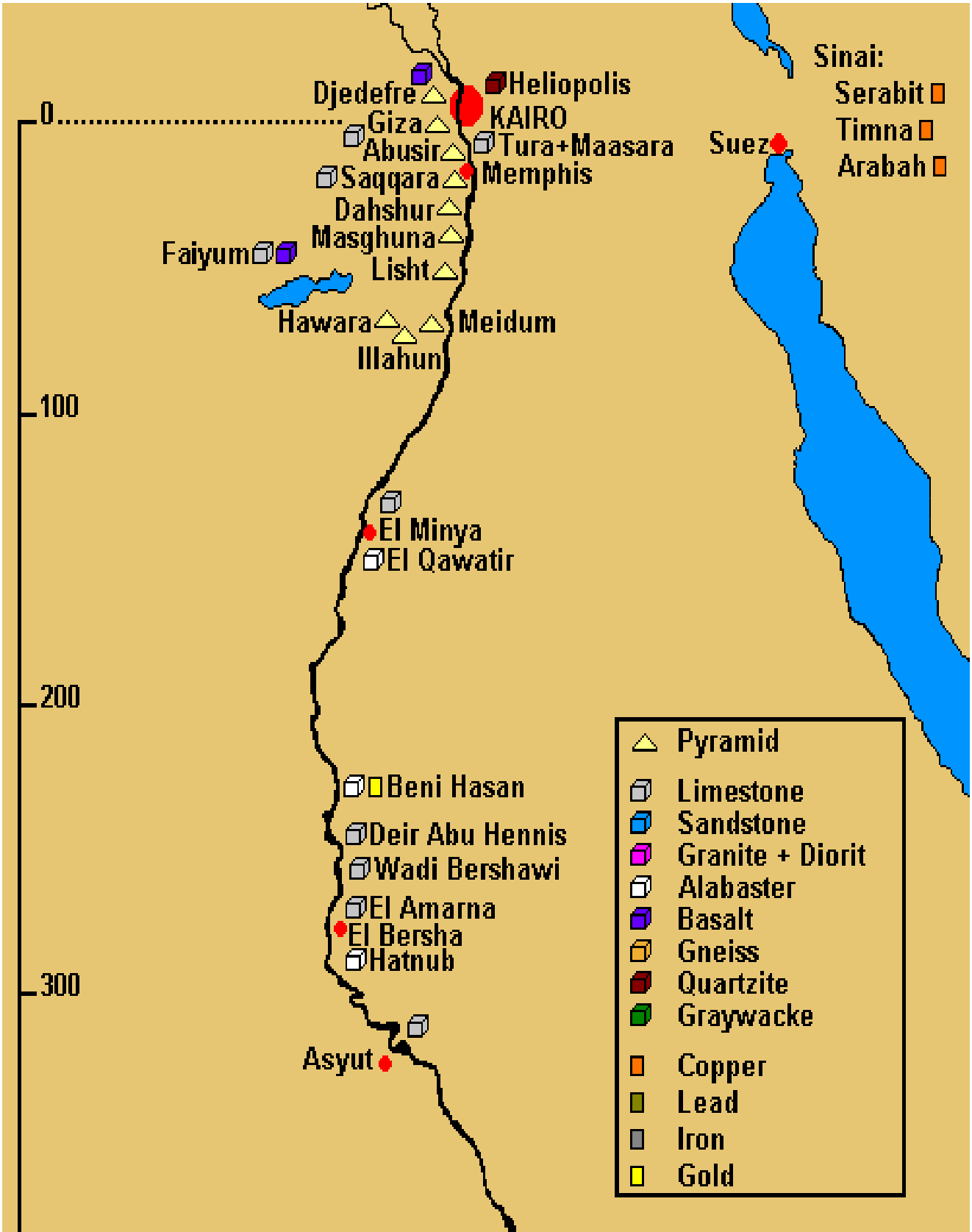

First pyramid (step pyramid) built for Pharaoh DJOSER by his architect IMHOTEP in Saqqara (Memphis) 2630-2605 b.c.

height: 62 m; base: 120/110 m

Rhomboid Pyramid of Sneferu (Dahshour)
(height: 105; base: 188/60)

Pyramids of Gizeh (Giza)

Pyramid of the Pharaoh Kheops (Khufu)
(initial heigh: 146 m; square base: 230 m)
(2584 bc……20-25 years.?)
2.5 million blocks, 2.5…60 tons

Senefru's bent Pyramid in Dahshour

Kenneth J.D. MacKenzie *et al*, Materials Letters, 65 (2011) 350

A: pyramid stone; B: Tura quarry limestone
C: Khufu quarry limestone; D: Diamaceous earth